JOURNAL OF NEUROPHYSIOLOGY
Vol. 70, No. 5, November 1993. *Printed in U.S.A.*

Tonotopic and Functional Organization in the Auditory Cortex of the Big Brown Bat, *Eptesicus fuscus*

STEVEN P. DEAR, JONATHAN FRITZ, TIM HARESIGN, MICHAEL FERRAGAMO, AND JAMES A. SIMMONS
Departments of Neuroscience and Psychology, Brown University, Providence, Rhode Island 02912

SUMMARY AND CONCLUSIONS

1. In *Eptesicus* the auditory cortex, as defined by electrical activity recorded from microelectrodes in response to tone bursts, FM sweeps, and combinations of FM sweeps, encompasses an average cortical surface area of 5.7 mm^2. This area is large with respect to the total cortical surface area and reflects the importance of auditory processing to this species of bat.

2. The predominant pattern of organization in response to tone bursts observed in each cortex is tonotopic, with three discernible divisions revealed by our data. However, although cortical best-frequency (BF) maps from most of the individual bats are similar, no two maps are identical. The largest division contains an average of 84% of the auditory cortical surface area, with BF tonotopically mapped from high to low along the anteroposterior axis and is part of the primary auditory cortex. The medium division encompasses an average of 13% of the auditory cortical surface area, with highly variable BF organization across bats. The third region is the smallest, with an average of only 3% of auditory cortical surface area and is located at the anterolateral edge of the cortex. This region is marked by a reversal of the tonotopic axis and a restriction in the range of BFs as compared with the larger, tonotopically organized division.

3. A population of cortical neurons was found (n = 39) in which each neuron exhibited two BF threshold minima (BF_1 and BF_2) in response to tone bursts. These neurons thus have multipeaked frequency threshold tuning curves. In *Eptesicus* the majority of multipeaked frequency-tuned neurons (n = 27) have threshold minima at frequencies that correspond to a harmonic ratio of three-to-one. In contrast, the majority of multipeaked neurons in cats have threshold minima at frequencies in a ratio of three-to-two. A three-to-one harmonic ratio corresponds to the "spectral notches" produced by interference between overlapping echoes from multiple reflective surfaces in complex sonar targets. Behavioral experiments have demonstrated the ability of *Eptesicus* to use spectral interference notches for perceiving target shape, and this subpopulation of multipeaked frequency-tuned neurons may be involved in coding of spectral notches.

4. The auditory cortex contains delay-tuned neurons that encode target range (n = 99). Most delay-tuned neurons respond poorly to tones or individual FM sweeps and require combinations of FM sweeps. They are combination sensitive and delay tuned. The response of cortical delay-tuned neurons is phasic with an average of 1.1 ± 0.6 (mean ± SD) action potentials per pulse-echo pair. Thus delay-tuned neurons act as coincidence detectors without additional facilitation.

5. The distribution of best echo delays (BDs) of cortical delay-tuned neurons appears bimodal, with neurons in the first mode (n = 33) encompassing BDs from 2 to ~11 ms and the second mode (n = 66) from ~11 to 28 ms. The distribution of BDs in the first mode is similar to the range of BDs seen in other species of bats, but the distribution of BDs encompassed by the second mode appears unique and suggests a longer working range for echolocation in this species. As an ensemble, cortical delay-tuned neurons encode target ranges of 34–484 cm, corresponding to the behaviorally observed 5-m limit for the detection of insect-sized objects.

6. Delay-tuned neurons in the tonotopically organized area (n = 36) typically exhibit shorter BDs and longer echo facilitation latencies (EFLs) than delay-tuned neurons in the variable frequency area (n = 48). These differences are statistically significant and suggest that delay-tuned neurons in the variable and tonotopic regions constitute separate, multiple representations of target range information.

7. The distribution of BDs of delay-tuned neurons is not topographically arrayed across the auditory cortex, at least not on the same large scale as tonotopic frequency organization.

8. Some (13 out of 25 tested) delay-tuned neurons systematically shifted their BDs in response to changes in the simulated pulse amplitude. These delay-tuned neurons are termed "amplitude shift" neurons. Of the 13 amplitude shift neurons, 11 exhibited a decrease in BD in response to decreasing pulse amplitudes, and 2 exhibited an increase in BD in response to decreasing pulse amplitudes. Amplitude shift cells shifted their BD by an average 11 ± 8 ms for an average change of 13 ± 8 dB SPL. The location of amplitude shift cells appears randomly distributed among delay-tuned neurons in the variable and tonotopic areas.

9. We develop a conceptual framework to understand the nontopographic organization of BDs by considering the overlapping multipeaked frequency-tuned and delay-tuned cortical fields in *Eptesicus* as parallel spectral and temporal components of a target range imaging process.

INTRODUCTION

Echolocating bats emit complex biosonar signals and analyze returning echoes for orientation and for location of prey. The big brown bat, *Eptesicus fuscus* (Kurta and Baker 1990), uses short multiharmonic sonar signals and extracts at least two different kinds of acoustic cues for target range from its biosonar echoes (Griffin 1958; Simmons et al. 1990). The first well-documented echolocation cue is the delay between each emitted biosonar signal or *pulse* and returning *echoes* for encoding target range (Simmons 1971, 1973, 1989), which is determined across many different frequencies contained in the signal. The second cue is contained in the interference spectrum of overlapping echoes reflecting from objects with complex surface geometries such as insects (Beuter 1980; Habersetzer and Vogler 1983; Kober and Schnitzler 1990; Simmons and Chen 1989). Behavioral experiments have shown that spectral notches contained in the interference spectrum alone are a sufficient biosonar cue for the perception or discrimination of multiple target ranges to different parts of a complex target (Habersetzer and Vogler 1983; Mogdans and Schnitzler 1990; Schmidt 1988, 1992; Simmons et al. 1990).

Every species of echolocating bat thus far studied contains cortical neurons specialized for encoding specific values of echo delay called delay-sensitive or *delay-tuned neurons* (Berkowitz and Suga 1989; Feng et al. 1978; O'Neill and Suga 1979; Schuller et al. 1991; Suga et al. 1978; Sullivan 1982; Wong and Shannon 1988). In the auditory cortex of the mustached bat, *Pteronotus parnellii parnellii,* delay-tuned neurons are clustered into three separate cortical fields: the FM-FM area, dorsal fringe (DF), and ventral fringe (VF) (Edamatsu et al. 1989; O'Neill and Suga 1979, 1982; Suga and Horikawa 1986; Suga and O'Neill 1979; Suga et al. 1978, 1983). The best echo delay (BD) for each field is systematically arrayed topographically across the surface of the cortex (Edamatsu et al. 1989; O'Neill and Suga 1979, 1982; Suga and Horikawa 1986; Suga and O'Neill 1979; Suga et al. 1978, 1983). *Pteronotus* emits biosonar signals with a long constant frequency component followed by a decreasing frequency-modulated sweep and is referred to as a CF-FM bat. In contrast to the pattern of cortical organization seen in *Pteronotus,* delay-tuned neurons in the auditory cortex of the phylogenetically distant little brown bat, *Myotis lucifugus,* do not appear to cluster into functionally homogenous subdivisions. Furthermore, BD tuning is not systematically arrayed across the cortical surface in this species (Wong and Shannon 1988). *Myotis* uses a simpler biosonar signal consisting of a decreasing frequency-modulated sweep (FM) and is referred to as an FM bat. Differences both in biosonar signals and in cortical organization of delay tuning suggest the possibility the CF-FM and FM bats are fundamentally different in the way they represent biosonar information.

Like *Myotis, Eptesicus* is an FM bat, yet in spite of extensive behavioral investigations on the perception and discrimination of target range in *Eptesicus* (Simmons 1973, 1979, 1989, 1992; Simmons and Chen 1989; Simmons et al. 1989, 1990) few electrophysiological studies on delay-tuned neurons have been performed in the auditory cortex of *Eptesicus* (Dear et al. 1990; Feng et al. 1978). In addition, neurons involved in encoding spectral interference cues underlying echolocation behavior have not been identified. The aim of the present research was to explore the functional organization of the auditory cortex in *Eptesicus* as a model of auditory processing of several biologically relevant features extracted from the same complex signals. Specifically, we studied the tonotopic and delay-tuned organization in the auditory cortex of awake bats because both the frequency composition and the delay of echoes have been shown to contribute to the perception of target range.

METHODS

Surgery and recording of neural responses

We recorded neural responses from 16 adult awake big brown bats, *Eptesicus fuscus,* collected from attics of houses in Rhode Island. The flat head of a 1.5-cm stainless steel post (Small Parts TS-80) was attached to the anterior portion of the skull with Loctite No. 411. Bats were kept isolated for 3 days after surgery and were given tetracyclinated water (200 mg/l) throughout the course of the experiment to prevent infection. Also to prevent infection, instruments, cotton balls, and cotton swabs were autoclaved, and sterile gloves were worn.

On experimental days the bat was placed in a specially designed restraint suspended at the center of a soundproof room (IAC 400 A). The walls of the room were covered with fireproof echo-attenuating foam (Sonex). The restraint was designed to provide an airspace around the bat's body and move when the bat moved. To immobilize the bat's head, the post mounted on the skull was locked into a brass rod with set screws. To admit recording and indifferent microelectrodes, 50- to 100-μm-diam holes were drilled into the skull with the aid of a sharpened, sterile sewing needle (No. 9) and visualized with a $\times$40 operating microscope (JENA 212T). Care was taken not to rupture the dura while drilling. A session for recording extracellular action potentials lasted $\sim$8 h during which the bat was offered water at 1-h intervals. It was possible to record from individual bats for up to 4 mo. Each bat was given at least 1 day of rest between recording sessions.

Acoustic stimulation

Three types of acoustic stimuli were presented to the bat: tone bursts, FM sweeps, and combinations of FM sweeps simulating biosonar vocalizations (pulse) and returning echoes. Tone bursts were generated by a sine-wave oscillator (Leader 27A) and fed through an electronic switch (Coulbourn S84–04, modified). Signal duration was fixed at 2 ms with a rise/decay time of 0.5 ms. Tone bursts were used to determine the tonotopic organization of the auditory cortex.

Individual FM sweeps and pulse-echo combinations were digitally synthesized with a two-channel arbitrary function generator (RC Electronics RC216) with 16-bit resolution and a 1-MHz digital to analog conversion rate. These signals were created from custom software and were loaded into the generator via an IBM PC/AT computer. An FM sweep consisted of two harmonics presented simultaneously. Each harmonic sweep consisted of a frequency hyperbolically decreasing with time. Frequencies in the first harmonic ranged from 50 to 25 kHz and 100 to 50 kHz for the second harmonic. The amplitude relation of the harmonics could be varied under computer control. These harmonically structured stimuli were designed to mimic components of the sonar signals of *Eptesicus.* FM sweeps were presented either individually or as combinations simulating outgoing pulses and returning echoes. All FM sweeps were 2 ms in duration with a Hanning amplitude envelope.

Combinations of pulses and echoes appeared in a sequence of 13 components: a single pulse, followed by 11 pulse-echo pairs followed by a single echo. The echo delay between successive pulse-echo pairs was decremented by a constant interval, simulating the pattern of echoes reflected by an approaching object. In this sequence, the starting echo delay interval, ending echo delay interval, and echo delay decrements were all under computer control. This stimulus pattern allowed rapid assessment of both the combination-sensitivity and best echo delay-tuning of neurons.

Timing for all stimulus presentations was digitally controlled by four programmable timers (RC Electronics RC204) via an IBM PC/AT computer. Custom software allowed on-line modification of the stimulus timing parameters. Stimulus repetition rates of 5/s were used.

Each channel (pulse and echo) from the arbitrary waveform generator was individually attenuated (HP 350D), mixed, amplified (Harmon/Kardon PM645), and delivered to an ultrasonic transducer (Technics 10TH1000). Second harmonic distortion of the ultrasonic transducer was <40 dB over the frequency range of 10–110 kHz. Third harmonic distortion was <55 dB. Acoustic stimuli were presented free-field with the ultrasonic transducer placed directly in front of the bat (0° azimuth, 0° elevation) at a distance of 47 cm from the bat's ears.

Data acquisition and processing

A 10-μm carbon-fiber microelectrode (Armstrong-James and Milnar 1979) was inserted into the cortex for recording action

potentials from single or multiple neurons. Most of the insertions were orthogonal to the cortical surface. An indifferent tungsten wire electrode was placed on the dura matter outside the boundary of the auditory cortex. Action potentials were differentially amplified (WPI DAM-05) and band-pass filtered (Rockland/Wavetek 442) and then fed into a window discriminator (custom built).

To identify action potentials from a single neuron or to help isolate action potentials from a single neuron in a multiple neuron recording typically containing two or three neurons, action potentials were also fed into an analog delay line (custom built) and then into an oscilloscope externally triggered by the output [transistor-transistor logic (TTL pulses)] of the window discriminator. In this configuration, only the action potentials triggered by the window discriminator were displayed. This allowed for optimal adjustment of the window discriminator to select action potentials from a single neuron.

The arrival time of discriminated action potentials were measured with a timer (Modular Instruments Incorporated M100 & M110) and fed into an IBM PC/AT for on-line and off-line display and processing of action-potential arrival times. On-line display and processing for all neurons included a real-time raster display of neuronal firing together with a simultaneous display of the resulting peristimulus time histogram (PSTH). Acoustic thresholds were determined audiovisually. Best frequencies (BFs) and amplitudes corresponding to the maximum neuronal response to tone bursts were measured. The best amplitudes for pulse-echo combinations were also measured. Action-potential arrival times were measured with a resolution of 0.1 ms for tone bursts and single FM sweeps with a spike count window of 800 ms. Action-potential arrival times were measured with a resolution of 0.4 ms for sequences of pulse-echo pairs with a spike count window of 2,600 ms. Both action-potential arrival times and PSTHs for all stimuli were saved to disk for off-line processing.

Off-line processing included the analysis of neural response latencies, determination of the numbers of stimulus-evoked action potentials, and quantification of the temporal firing characteristics from single-unit recordings of delay-tuned neurons. Response latencies were measured from cumulative PSTHs formed by integrating individual PSTHs and determining the first stimulus-evoked change in firing rate. The latency of a facilitative response to a pulse-echo pair was always measured either from the onset of the pulse [*pulse facilitation latency* (PFL)] or echo [*echo facilitation latency* (EFL)]. The acoustic delay due to the conduction time from the ultrasonic transducer to the bat's ear, 1.4 ms, was subtracted from these recorded latencies. The number of stimulus-evoked action potentials was determined by two methods: by counting the number of action potentials evoked by the stimulus from cumulative PSTHs collected at BD, best pulse amplitude, and best echo amplitude or by counting the number of action potentials in the PSTHs following the stimulus-evoked response until a 4-ms gap without neural activity was encountered. Both methods yielded similar results. The temporal firing characteristics of single-unit recordings of delay-tuned neurons were determined by computing the standard deviation of action-potential arrival times in PSTHs following the stimulus-evoked response until a 4-ms gap without neural activity was encountered.

Construction of composite maps

To determine the tonotopic and delay-tuning organization of the auditory cortex, both individual and composite maps of response properties were constructed (O'Neill and Suga 1982; Suga and Manabe 1982). Because the skull of the bat is translucent, the cortical surface is clearly visible. We sketched the cortical blood vessel pattern for each bat with the aid of an ocular micrometer in the operating microscope. Each electrode penetration was indicated on the sketch, and the stimulus parameters that elicited the maximum response from neurons in each penetration (such as BF, best amplitude, and BD) were recorded. Individual maps were drawn for each bat.

To better judge the correspondence of the tonotopic organization to the delay-tuned organization, composite maps for BF and delay tuning were constructed in the following manner. Only individual BF maps that were relatively complete and similar in organization to one another were used to construct the composite map, and individual maps were added into the composite by the use of best frequencies and the middle cerebral artery as guides for alignment. Thus only 10 out of a total of 16 maps were used in the composite BF map. Next, BF values were digitized along with associated coordinate data from the composite BF map. A distance-weighted least-squares algorithm (Systat, V 5.0) was used to generate isofrequency contours in integer multiples of 10 kHz on top of the composite map. Thus the computer-generated isofrequency map represented a spatial average of individual BF maps. In the extreme, spatial averaging of data with high variance can have the result of generating a composite map with no correspondence to individual maps. To minimize this possibility, we took the additional step of color coding the composite BF points by giving frequencies within a 10-kHz-wide band a different color. The color coding was compared with the isofrequency contours. With the use of this comparison, map regions with considerable variance of BF were apparent. Our choice was to define regions of high variance as containing many neurons with >10-kHz differences. Given the distinctly higher variance of one specific cortical region, our arbitrary threshold was conservative.

Some neurons responded to two different ranges of tone bursts and were called multipeaked frequency-tuned neurons. A composite map of the spatial distribution of multipeaked frequency-tuned neurons was constructed with the use of 5 of the 10 animals used for the composite BF map. The *identical* alignments between the *same* individual animal maps used to construct the composite BF map was also used to construct the composite multipeaked map.

A composite map of the spatial distribution of delay-tuned neurons was constructed with the use of 8 of the 10 animals used for the composite BF map, and the *identical* alignments between the *same* individual animal maps used to construct the composite BF map were also used to construct the composite delay-tuned map. The practical consequence of the construction of the composite maps is twofold and will be discussed in greater detail in RESULTS. First, composite maps provide a conservative estimate of the location and extent of the auditory cortex. Second, the distribution of multipeaked neurons can be compared with the distribution of delay-tuned neurons, and both distributions can be compared with the tonotopic organization in this species.

RESULTS

Location and extent of auditory responses

We first determined the location and extent of the auditory cortex with the use of tone bursts as well as individual and paired FM sweeps, by mapping electrode recording sites onto a sketch of the cortical surface for each hemisphere. We recorded a total of 653 neurons that responded to acoustic stimuli in the cortices of 16 awake bats. Single- and multiunit responses were recorded at depths ranging from 200 to 950 μm below the cortical surface, with the majority of responses encountered at depths between 300 and 850 μm. We used a minimum depth separation of 75 μm between successive units and recorded an average of three units/penetration. We recorded up to seven units in a single electrode penetration.

Electrode penetrations containing neurons responding to acoustic stimuli clustered together into a single, posterolat-

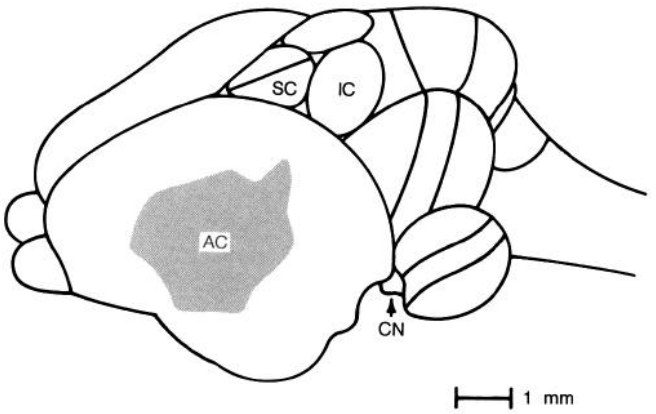

FIG. 1. Dorsal-lateral view of the brain of the big brown bat, *Eptesicus fuscus*. Auditory areas include the cochlear nucleus (CN), inferior colliculus (IC), and superior colliculus (SC). Shaded area defines a conservative estimate of the location and extent of the auditory cortex (AC) as determined from single- and multiunit recordings obtained in this study.

eral region of the neocortex for each map. Determination of the perimeter of the auditory cortex for individual maps was complicated by several factors. Not all of the cortices were mapped to completion because of premature death, cerebrovascular accidents or the inability to expose all the cortex for recording in certain bats. The latter factor proved to be the greatest hindrance in determining the ventral extent of the auditory cortex.

Given the uncertainties associated with estimating map perimeters and variations in BF distributions for individual bats, we chose the strategy of estimating the location and extent of the auditory cortex by constructing a composite map with responses pooled from individual maps (see METHODS). It is well documented that this procedure can produce errors when used to estimate the topographic distribution of response properties such as BF (Merzenich et al. 1975), but this procedure has been effectively used in bats (O'Neill and Suga 1982; Suga and Manabe 1982). Figure 1 shows the extent and location of the auditory cortex as estimated by the composite map. As expected from the behavioral importance of echolocation for *Eptesicus,* the auditory cortex occupies a large portion of the total cortical surface area. The composite cortical surface area of 5.7 mm^2 is smaller than some individual maps and overall represents a conservative estimate of the total extent of the auditory cortex.

Columnar organization of BFs

The systematic organization of neural responses to a particular stimulus dimension across the cortical surface implies systematic organization along cortical depth as well, and this is referred to as columnar organization. We investigated the columnar organization of neuronal BFs across the entire auditory cortex for electrode penetrations containing two or more successive neurons responsive to acoustic stimuli by considering both the absolute frequency differences and the relative frequency differences among BFs of neurons within each penetration. A histogram of the distribution of values representing the absolute frequency difference in kilohertz between the maximum and minimum BFs in a single-electrode penetration for 118 penetrations is shown in Fig. 2. Difference frequencies ranged from 0 to 44.5 kHz with an average of 4.5 ± 7.0 kHz. The number of penetrations in the histogram bins decreased monotonically for frequency differences of 0–12 kHz. Above 12 kHz, the number of penetrations per bin remain approximately constant for frequency differences up to 30 kHz.

A variation in BF of 5 kHz in a penetration with BFs around 95 kHz implies columnar organization of BF, whereas the same variation in a penetration with BFs around 10 kHz does not imply columnar organization. To minimize this problem, we also computed the ratio of the maximum BF to the minimum BF for the same 118 penetrations. The distribution of ratios ranged from 1.00 to 2.43 with an average of 1.12 ± 0.20. Similar to the comparison of BF differences in Fig. 2, the number of penetrations in the distribution decreased monotonically for ratios of 1.00–1.25. This monotonic decrease may reflect, in part, our inability to always make perfect orthogonal electrode penetrations. However, because the number of penetrations remained approximately constant for BF ratios between 1.25 and 1.70, the BFs in some penetrations were noncolumnar. These data demonstrate some diversity in the correspondence of BFs within a single penetration but suggest that the majority of penetrations exhibited columnar organization.

Representation of frequency in auditory cortex

The investigation of frequency representation in the auditory cortex of this species is complicated by the small absolute cortical size, number of blood vessels, and wide range of behaviorally relevant frequencies. Also, electrode penetrations necessarily were positioned between blood vessels, resulting in a somewhat uneven pattern of recording sites.

Cortical maps for three animals illustrating the typical representation of frequency are shown in Fig. 3, *A–C*. In the maps from *animals E31090R* and *E31390R,* the lowest BFs defined the posterior extent of the auditory cortex. However, this was not true for *animal E51490R*. There is a

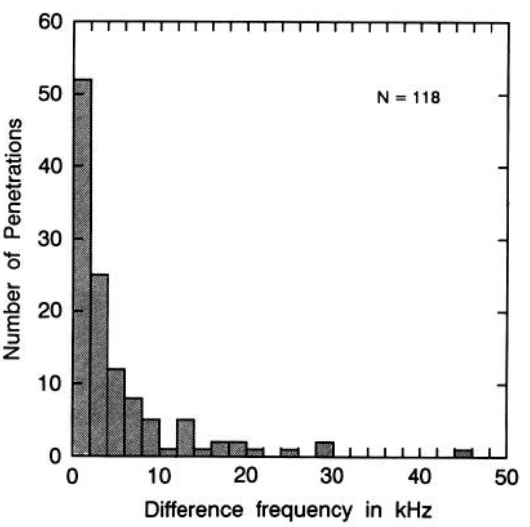

FIG. 2. Histogram comparing the differences in best frequency (BF) for neurons responding to single tone bursts encountered in single-electrode penetrations. These data illustrate the columnar organization of BF in the cortex. Electrode penetrations (n = 118) were collected where BFs of 2 or more were neurons were characterized. Abscissa gives the largest difference in BF (kHz) among neurons successively encountered in each penetration. Successive recordings from neurons in individual electrode penetrations were at least 75 μm apart in depth.

suggestion of an increasing BF along the ventroposterior-dorsoanterior axis in all three animals, but the progression of BF with location is not "strictly" tonotopic.

BFs in the anterior half of the auditory cortex varied widely. In particular, *animal E31390R* exhibited BFs from 19 to 82 kHz. BFs at the anterior border are low in all three animals, suggesting a reversal in the direction of the frequency axis in this area.

To better judge the tonotopic organization, the same method of pooling individual cortical maps into a composite map that was used in estimating the extent and location of the auditory cortex was also used to construct a composite BF map (see METHODS). The resulting cortical organization of the composite map is shown in Fig. 4. On the basis of location and variation of BFs, we divided the auditory cortex into three regions: A, B, and C. The posterior portion of cortex in the composite BF map, A, exhibits clear tonotopic organization with a systematic decrease in BF along the anterioposterior axis. The shaded area, B, is a highly variable region where no consistent tonotopic organization across animals was observed, although some individual bats do show tonotopy in this area. A small third region, C, is found at the anterior border of the auditory cortex. The region is characterized by a reversal of tonotopic organization as compared with the first region. The range of BFs is restricted to a range of 50–20 kHz in the third region.

The composite BF map can also be used to examine the relationship between the frequency representation in the brain in relation to the biosonar signals used by *Eptesicus*. Spectrograms of typical *Eptesicus* biosonar signals recorded in the laboratory as a volant bat approaches and attacks a stationary microphone are illustrated in Fig. 5, *a–g*. All the spectrograms in the pursuit sequence share the common feature of containing harmonic structure. Each harmonic consists of a curvilinear logarithmically or hyperbolically decreasing frequency sweep and contains the frequency content typically reported in the literature (Brigham et al. 1989; Gould 1971; Griffin 1958, 1962; Jen and Kamada 1982; Masters et al. 1991; Thomas et al. 1987). When the bat is ≤50 cm from the microphone, a fourth harmonic (FM_4) is produced, and the lower-frequency limit of FM_1 drops to <15 kHz (Fig. 5, *E–G*).

The percent normalized cortical surface area associated with each 10-kHz frequency interval is presented in Table 1. If the cortical surface area associated with specific frequencies were distributed proportionally across the bandwidth of 10–90 kHz, then the area associated with each 10-kHz interval of the total bandwidth should encompass ~12% of the total area, and intervals encompassing areas >12% suggest possible cortical overrepresentation. The predicted percentage of cortical area associated with frequencies of 20–50 kHz in the tonotopically organized area A is 38%, and the actual area of 74% is disproportionately overrepresented and may represent the importance of FM_1 to the bat. Area C also corresponds to the frequency range of FM_1.

Latency of responses to tone bursts

For the purpose of comparison with delay-tuned neurons, we determined the latencies of some neurons not specialized for delay tuning from PSTHs with tone-burst stimuli adjusted in frequency and amplitude to elicit a maximum response. Response latencies of the unspecialized neurons (n = 221) varied from 6.4 to 36.1 ms with a mean of 13.8 ± 5.7 ms. The distribution of response latency varied as function of BF and is shown in Fig. 6. Short to moderate latencies were found at all BFs, whereas the longest latencies were associated with BFs between 25 and 50 kHz, corresponding to the frequency range of FM_1 (Fig. 5). A second increase in latency is associated with BFs between 55 and 70 kHz, corresponding to the frequency range of FM_2. Interestingly, BFs between 50 and 55 kHz were almost absent, leaving a sharp gap in the distribution of BFs.

Multipeaked frequency threshold tuning of neurons

Another characterization of neural responses to tone bursts is the frequency threshold tuning curve. The BF data corresponding to the threshold minima of the frequency threshold tuning curve already exist for *Eptesicus* (Jen et al. 1989). Consequently, in our experiments, frequency threshold tuning curves were not routinely recorded as part of our characterization of neurons to tone bursts, except for occasional neurons with unusual frequency tuning characteristics. *Neuron E51490R-31-1* (Fig. 7*A*) exhibits a frequency threshold tuning curve with two separate threshold minima. The two BFs corresponding to the threshold minima of this neuron, BF_1 = 22 kHz and BF_2 = 89 kHz, are unusual in that the BF_2/BF_1 ratio is harmonic with a four-to-one relationship. For *neuron E51890R-12-1* (Fig. 7*B*) the two BFs associated with the threshold minima, BF_1 = 15 kHz and BF_2 = 45 kHz, exhibited a more common harmonic BF_2/BF_1 ratio with a three-to-one relationship.

A total of 39 multipeaked frequency-tuned neurons were recorded in this study, and BF_2/BF_1 ratios for these neurons are summarized in Fig. 7*C*. All but one of these multipeaked neurons were not delay tuned, and BF_1s ranged from 9.6 to 48.3 kHz with a mean of 20.4 ± 7.3 kHz, and BF_2s ranged from 28.0 to 91.0 kHz with a mean of 58.7 ± 16.8 kHz. The sloping lines shown in this figure represent BF_2/BF_1 ratios of 1.5, 2, 3, and 4. The majority of neurons (n = 27) exhibit ratios that cluster around 3 ($2.5 \leq BF_2/BF_1 \leq 3.5$).

Multipeaked frequency tuning of neurons has been found in other mammalian species (Abeles and Goldstein 1970; Oonishi and Katsuki 1965; Suga and Manabe 1982; Suga and Tsuzuki 1985; Sutter and Schreiner 1991). We compared the distributions of BF_2/BF_1 ratios for *Eptesicus* and cat to gain insight into the hypothesis that multipeaked neurons in different species may be part of a common signal processing mechanism. Figure 8 illustrates histograms of the distributions of BF_2/BF_1 ratios of multipeaked neurons from *Eptesicus* and cat (Sutter and Schreiner 1991). BF ratios in *Eptesicus* ranged from 1.6 to 5.2 with a mean of 2.5 ± 0.8. Stars in both histograms identify integer harmonic ratios. Whereas the majority (69%) of multipeaked neurons in *Eptesicus* cluster around ratios of 3, only 10% of multipeaked neurons in cat clustered around this ratio. Furthermore, the majority of multipeaked neurons in cat clustered around ratios of 1.5, whereas only 3% of the multipeaked neurons in *Eptesicus* clustered around this ratio. We used the nonparametric Kolmogorov-Smirnov two-

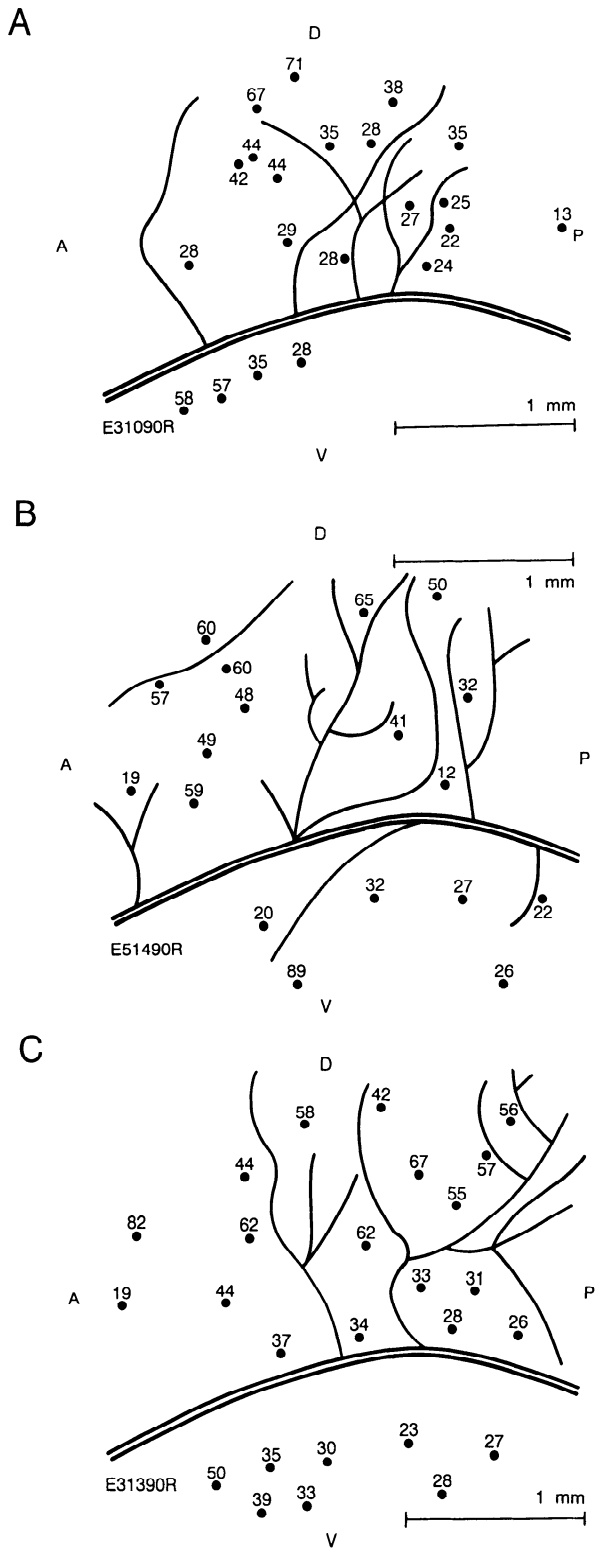

FIG. 3. Examples of individual BF maps from the right auditory cortices of 3 bats. The 2 dimensions represent the dorsal-ventral (D, V) and anterior-posterior (A, P) extent of the cortical surface. Circles represent orthogonal electrode penetrations, and each number associated with an electrode penetration is an average of the BFs that evoked the maximum neural firing for each neuron in the penetration. BFs are reported in kilohertz. Double lines represent the middle cerebral artery, whereas single lines represent branching arteries. Individual maps suggest the typical mammalian pattern of tonotopic organization, with high frequencies decreasing to low along the anterior-posterior axis. These examples also reveal considerable variability across individual bats.

sample test of unequal size to evaluate the probability that both sample distributions were from a common population, suggesting a common functional role of multipeaked tuning. This test was chosen because it is conservative (tends to accept the null hypothesis), nonparametric, and works well for discontinuous distributions. The difference between the two distributions was significant (Systat, V 5.0, $D = 0.73$, $P < 1.2 \times 10^{-7}$).

We compared the spatial distribution of threshold BFs of multipeaked frequency-tuned neurons in the cortex against the composite cortical BF organization. Results of this comparison from 5 of the 10 bats used in the construction of the composite BF map (Fig. 4) are shown in Fig. 9. Multipeaked neurons ($n = 21$) were found in the variable area (■, $n = 12$) and the high-frequency portion of the tonotopic area (●, $n = 9$). In general, there were little data to evaluate the possibility of a systematic correspondence between the BF_1s or BF_2s of multipeaked frequency-tuned neurons and BFs from the composite map. Also, the relationship between threshold BFs and the BF or BFs eliciting the maximum response is not known for individual neurons. In the tonotopic area, five of the multipeaked frequency-tuned neurons exhibited a BF_1 (asterisk), and one multipeaked frequency-tuned neuron exhibited a BF_2 (asterisk) between ±5 kHz of the composite map BF. For each of the six neurons, the threshold BF corresponding to the composite map BF also exhibited the lower amplitude threshold. A similar comparison could not be made for neurons in the variable area because the composite map BF was variable. However, several penetrations in the variable area contained multipeaked frequency-tuned neurons with BF_1s <20 kHz ($n = 7$) with a lower limit of 9.6 kHz. Typically, such low frequencies are only emitted during the terminal stage of echolocation (Fig. 5).

We investigated the columnar organization of multipeaked frequency-tuned neurons by comparing the BF_1 and BF_2 threshold frequencies in penetrations containing more than one neuron. A total of seven penetrations contained more than one multipeaked neurons (Table 2). Variations in BFs were normalized by computing the ratios of the maximum divided by minimum of BF_1s and BF_2s for each penetration. BF_1 ratios ranged from 1.00 to 2.49 with an average of 1.40 ± 0.56, and BF_2 ratios ranged from 1.00 to 2.81 with an average of 1.31 ± 0.67. However, much of the variation comes from two penetrations: *E2290R-16* and *E5290R-16*. The remaining five penetrations exhibit small variations between maximum and minimum BFs, suggesting that BFs in these penetrations show columnar organization for both BFs.

Combination sensitivity and delay tuning

Of the 653 neurons recorded in this study, 99 neurons were delay tuned. The data were obtained with computer-synthesized FM signals (see METHODS). The stimulus parameters yielding the maximum neural response were the best pulse amplitude (PBA), best echo amplitude (EBA), and BD. Examples of combination-sensitive, delay-tuned responses for four typical cortical delay-tuned neurons are presented in Fig. 10. All four neurons responded weakly to

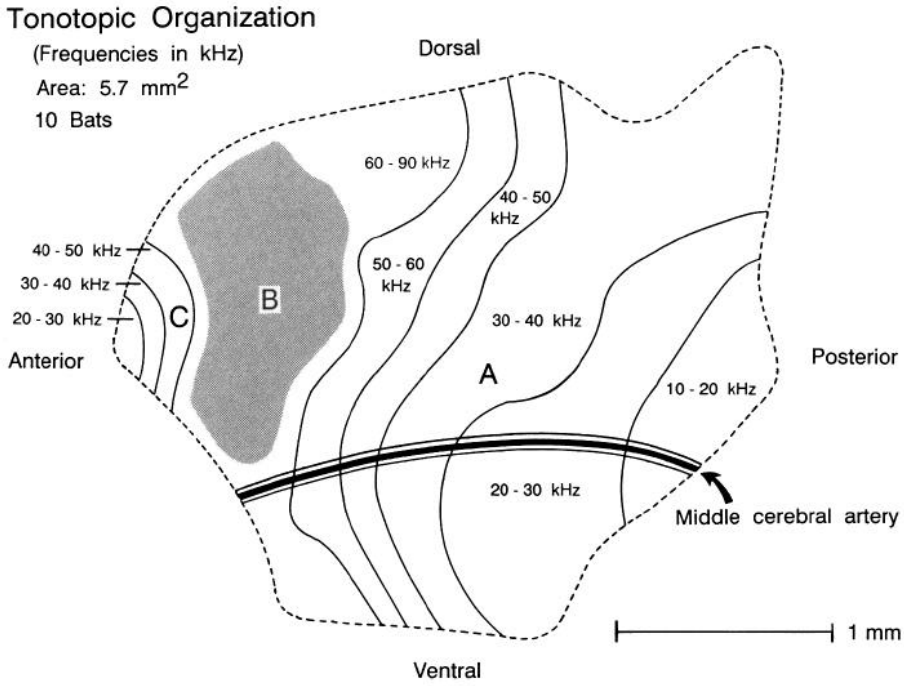

FIG. 4. Composite cortical map representing the neuronal BF responses to tone bursts. Lines on the cortical surface represent computer-generated isofrequency contours in frequency intervals of 10 kHz. Numbers bounded by contour lines represent BF values in kilohertz. Cortical BF maps from 10 of the 16 bats were used to construct the composite map. Area A exhibits tonotopic organization and corresponds to the organization observed in primary auditory cortex in other mammals, with high frequencies decreasing to low along the anterior-posterior axis. Area B (shaded) corresponds to a highly variable region where the frequency organization was quite different from animal to animal. This variable region may extend further ventrally. Area C contains a reversal in the tonotopic axis with high to low frequencies running along the posterior-anterior axis and may partially extend into Area B.

an individual pulse (PFM) or echo (EFM), whereas the combination of both components at BD, PBA, and EBA greatly increased or facilitated the number of impulses. All 99 delay-tuned neurons exhibited a facilitated response to a FM pair that was larger than the sum of the individual responses to PFM and EFM alone. The probability of discharge for all delay-tuned neurons depended on the value of echo delay between the PFM and EFM in the pair. Neural response magnitudes to delay values greater or less than the maximum facilitated response at BD diminished to a level similar to the summed response of PFM and EFM presented individually.

Representation of echo delay in auditory cortex

The spatial distribution of delay-tuned neurons over the auditory cortex appears relatively broad. Examples of cortical delay-tuning maps representing the spatial distribution of delay-tuned neurons are shown for four animals in Fig. 11, *A–D*. The majority of delay-tuned neurons in these four

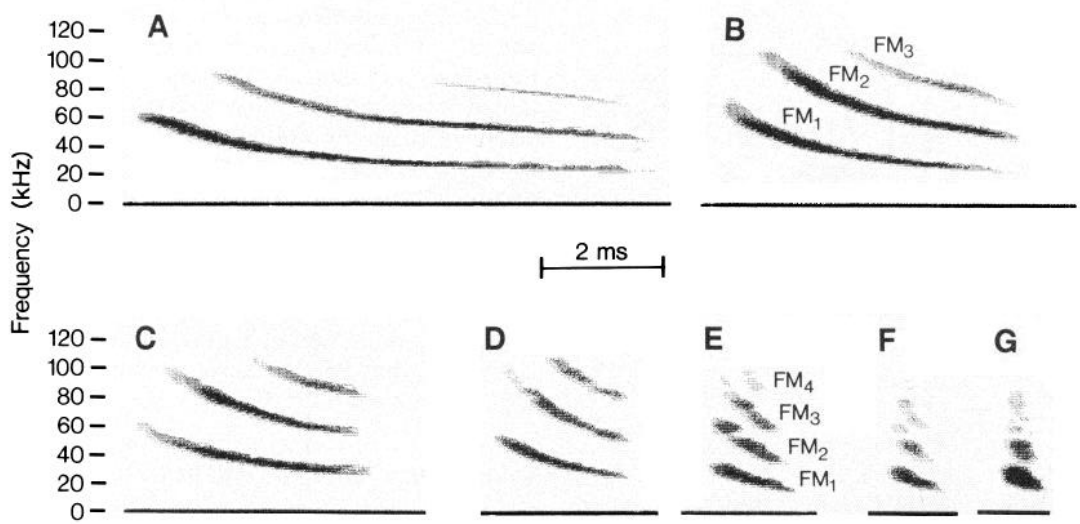

FIG. 5. *A–G*: sequence of spectrograms of typical biosonar signals of *Eptesicus* recorded from a flying bat approaching a stationary microphone. Each signal typically contains up to 4 harmonics, with each harmonic consisting of a decreasing, frequency modulated (FM_{1-4}) component. Typically, the 1st harmonic (FM_1) sweeps from 60 to 25 kHz, and the 2nd harmonic (FM_2) from 80 to 60 kHz. The 3rd harmonic sweeps (FM_3) from 100 to 85 kHz. The onset of the 2nd and 3rd harmonics are delayed from the onset of the 1st harmonic. Furthermore, as the bat approaches the microphone, the duration of the vocalization systematically decreases. *E–G*: at distances of ≤50 cm, the bat enters the terminal stage of echolocation behavior, which is characterized by both a dramatic increase in the vocalization rate (up to 180 vocalizations/s) and a decrease in both the vocalization duration and amplitude. In addition, these spectrograms recorded during the terminal stage show a decrease in frequency of the 1st 3 harmonics and the addition of a 4th harmonic.

TABLE 1. *The percent normalized cortical surface area associated with each 10-kHz frequency interval in the tonotopic area*

Frequency, kHz	%Area
Area A	
10–20	7
20–30	19
30–40	24
40–50	9
50–60	10
60–90	15
Area B	13
Area C	3

bats were found in the anterior half of the auditory cortex. *Bat E31390R* (Fig. 11*B*) represents an extreme case of asymmetry in spatial distribution with only 7 delay-tuned neurons in 3 penetrations in the anterior auditory cortex out of a total of 26 penetrations contained neurons responding to auditory stimuli. Yet, in spite of the asymmetry in the spatial distribution in this bat, delay-tuned neurons do not appear to form a separate homogenous cortical subdivision. For example, in *bats E31390R* (Fig. 11*B*) and *E6490L* (Fig. 11*C*), penetrations containing delay-tuned neurons were found to lie along a narrow strip. In *bat E31090R* (Fig. 11*A*) the distribution of penetrations containing delay-tuned neurons appears circular, surrounding penetrations containing no delay-tuned neurons.

Bat E51490R (Fig. 11*D*) represents the best example of a cortical map with the suggestion a BD axis. The BD axis is localized to the dorsoanterior region of the cortex (variable area, Fig. 4). Maps from three other bats have at least five penetrations containing delay-tuned neurons: *E31090R* (Fig. 11*A*), *E5290R*, and *E6490L* (Fig. 11*C*). There is the suggestion of topographic organization of BD in these three bats, but the orientation of this organization differed from bat to bat, and the total number of delay-tuned neurons recorded in these bats was small.

To gain insight into the delay-tuned organization of the auditory cortex, we constructed a composite delay-tuned map using most of the *same* bats and the *identical* alignment that was used in constructing the composite BF map. The resulting composite map of the spatial distribution of delay-tuned neurons ($n = 84$) from eight bats allowed us to superimpose BD data on the composite BF map as shown in Fig. 12. Delay-tuned neurons were found in both the tonotopic area (area A, Fig. 4) and variable area (area C, Fig. 4) of the auditory cortex but were not found in the small anterior region exhibiting a reversal in the tonotopic axis (area C, Fig. 4). The composite delay-tuning map suggests that there is no global systematic variation in BD as a function of location on the cortical surface.

The lack of a gross systematic axis for delay-tuning can be seen in Fig. 13. BD values were digitized along with associated coordinate data from the composite BD map (Fig. 12). A distance weighted least-squares algorithm (Systat, V 5.0) generated iso-BD contours in integer multiples of 2 ms. The orientation of the iso-BD contours does not reflect any pattern of *global* symmetry (parallel contours, radial contours, etc.). Because the composite BF map (Fig. 4), constructed from the *same* cortical maps with the *same alignment* as the composite BD map (Figs. 12 and 13), did exhibit systematic tonotopic organization, the absence of delay-tuning topography on a comparable scale probably is not a consequence of misregistration of electrode penetrations between individual cortical maps. Local topographic organization of BDs on a smaller scale is conceivable, however, and *bat E51490R* (Fig. 11*D*) raises the possibility of topographic organization of BD in the variable area (Fig. 12).

Figure 14 shows a histogram of the distribution of cortical BDs. The 99 delay-tuned neurons recorded in this study encompassed BDs of 2–28 ms, corresponding to target ranges of 0.35 to almost 5 m. The maximum physiologically determined range of 5 m corresponds to the maximum range at which the big brown bat can behaviorally detect insect-sized objects at 3–5 m (Kick 1982; Kick and Simmons 1984). The histogram in Fig. 14 also contains a gap in the distribution (star) for BDs between 6 and 15 ms. These data suggest that the distribution of cortical BDs is bimodal. One potential explanation of the gap is that BDs were not sampled with enough temporal resolution; that is, the gap just represents a sampling bias. However, this gap is more than a factor of two greater than the largest delay step interval (see METHODS). Possibly the auditory cortex of contains delay-tuned neurons with BDs corresponding to the gap, but for pulse repetition rates not tested here.

BDs of neurons ($n = 48$) in the variable area ranged from 2 to 28 ms with an average of 14.4 ± 5.4 ms. BDs of neurons in the tonotopic area ($n = 36$) ranged from 3 to 24 ms with an average of 9.9 ± 6.6 ms. Thus, although the extreme ranges represented by longest BDs of the two areas are similar, the distribution of BDs is different, with the tonotopic area containing a greater proportion of delay-tuned neurons having short BDs. The difference in BD distribution between these two areas was significant (Systat, V 5.5, *t* test, $t = 3.50$, df = 82, $P < 0.001$).

Temporal response properties of delay-tuned neurons

In addition to characterizing each neuron's ability to encode target range and recording its cortical location, we observed the temporal firing properties of delay-tuned neu-

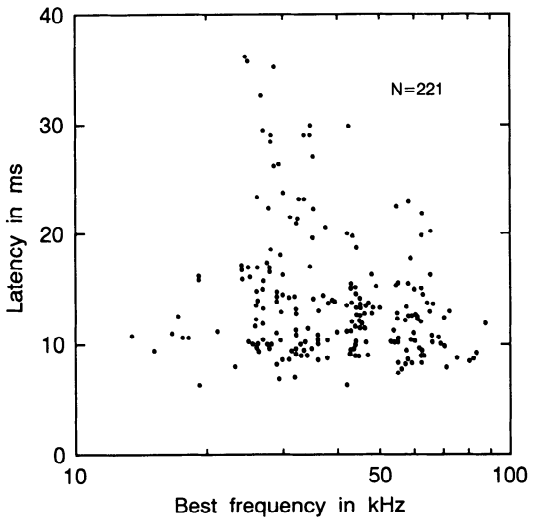

FIG. 6. Relationship between the cortical response latency and BF of individual neurons (●, $n = 221$).

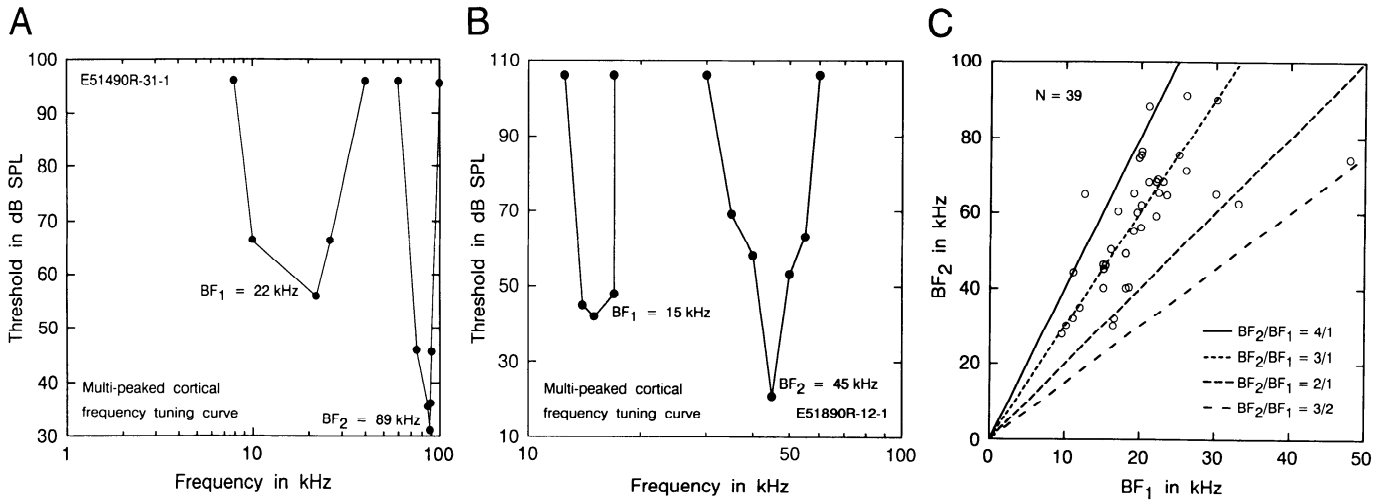

FIG. 7. *A*: multipeaked frequency threshold tuning curve for *neuron E51490R-31-1* that responded to 2 different frequency ranges. The threshold best frequencies, BF_1 = 22 kHz and BF_2 = 89 kHz, exhibit a harmonic ratio of 4-to-1. *B*: multipeaked frequency threshold tuning curve for *neuron E51890R-12-1*. The threshold BFs for this neuron, BF_1 = 15 kHz and BF_2 = 45 kHz, exhibit a harmonic ratio of 3-to-1. *C*: ratios between the upper and lower BFs for the multipeaked neurons (n = 39) recorded from this study. The different lines represent possible different harmonic ratios between the BFs, and as can be seen, the majority of multipeaked neurons exhibited ratios of ~3-to-1. Only 1 out of the 39 multipeaked neurons exhibited delay tuning.

rons. The PSTHs in Fig. 10 suggest that cortical delay-tuned neurons discharge phasically in response to paired stimuli. We investigated this question using data obtained from well-isolated, single-unit recordings of 33 delay-tuned neurons. The simulated pulse and echo amplitudes were adjusted for each neuron to yield a maximum firing rate (see METHODS), and a histogram of the distribution of number of impulses elicited by 50 pulse-echo stimuli for the 33 single-unit delay-tuned neurons is shown in Fig. 15. The number of stimulus-evoked impulses ranged from 15 to 154 with an average of 56 ± 29 imp/50 stimulus pairs. This is an average of 1.1 ± 0.6 imp/stimulus pair. The temporal jitter from discharge to discharge averaged 2.7 ± 2.4 ms. Thus cortical delay-tuned neurons typically discharge phasically with about one action potential per pulse-echo pair.

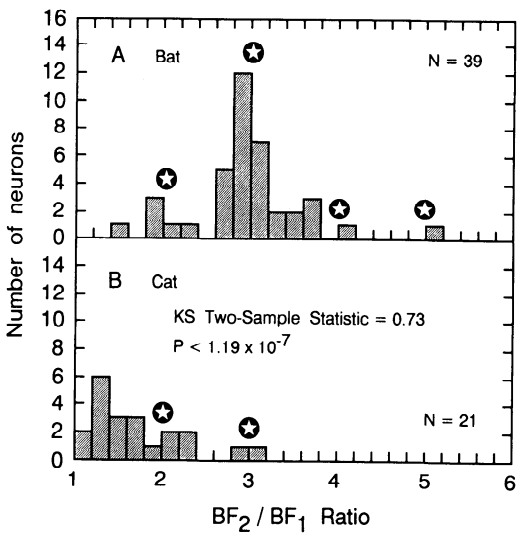

FIG. 8. Histogram representing the BF ratios of multipeaked frequency-tuned neurons recorded in *Eptesicus* is compared with a histogram representing BF ratios of multipeaked frequency-tuned neurons recorded in the cat (Sutter and Schreiner 1991). Stars identify integer harmonic ratios. Most multipeaked neurons in the bat exhibit integer harmonic ratios clustered around 3-to-1, whereas multipeaked neurons in the cat exhibit ratios mostly around 3-to-2. The distributions represented by the histograms were significantly different.

Delay-tuned neurons respond to the reception of an echo arriving at a specific time interval after the vocalization. It thus responds to a *pair* of sounds in a specific temporal relation. Neural response times or latencies for a delay-tuned neuron can be measured from the onset of either the pulse or the echo to the start of the neural response as determined from the PSTH. Figure 16*A* illustrates the timing relationships for the PFL and the EFL. The PFL represents the time from the onset of the simulated biosonar vocalization to the first occurrence of a neural discharge encoding target range information in the cortex. Figure 16*B* shows a histogram of the distribution of PFLs of 99 cortical delay-tuned neurons. PFLs ranged from 9.1 to 42.4 ms with an average of 25.0 ± 7.2 ms. A maximum PFL of 42.4 ms implies that target range information encoded by delay tuning persists in the cortex for a time covering the interval from one biosonar vocalization to the next for emissions at rates up to ~25 signals per second, which typically occur during the search, approach, and tracking stages of insect pursuit (Kick and Simmons 1984).

The EFL is the time from the onset of an echo to the first occurrence of a neural discharge encoding target range information in the cortex. Figure 16*C* shows a histogram of the distribution of EFLs of 99 cortical delay-tuned neurons. EFLs ranged from 5.6 to 34.4 ms with an average of 12.1 ± 5.5 ms. The dispersion of EFLs to such long intervals implies that the response of some delay-tuned neurons in the cortex is delayed with respect to other delay-tuned neurons for the same BDs. The distribution of EFLs is similar to response latencies of neurons unspecialized for delay tuning (6.4–36.1 ms with a mean of 13.8 ± 5.7 ms, Fig. 6). The overlap of latencies for delay-tuned and nondelay-tuned responses indicates that these different kinds of acoustic in-

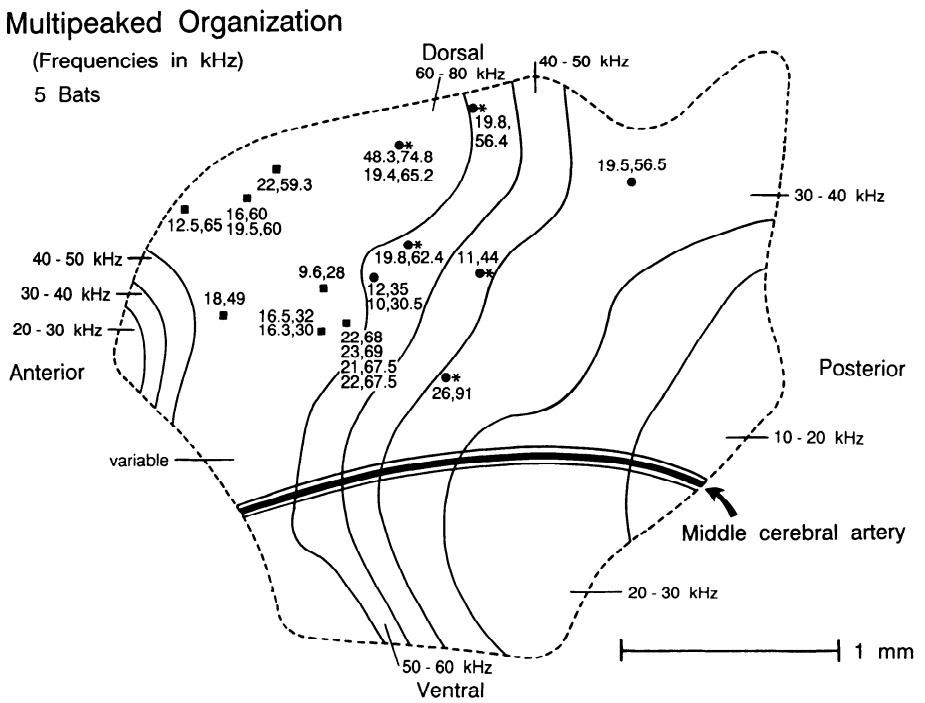

FIG. 9. Composite spatial representation of multipeaked frequency-tuned neurons from 5 bats, superimposed on the isofrequency contours of the composite tonotopic map from 10 bats (Fig. 4). Electrode penetrations containing multipeaked frequency-tuned neurons ($n = 21$) were found in the variable area (■, $n = 12$) and the high-frequency portion of the tonotopic area (●, $n = 9$). Pairs of numbers separated by commas represent threshold BFs (BF_1, BF_2) of multipeaked frequency-tuned neurons in kilohertz, and multiple pairs in a single penetration represent sequential multipeaked neurons encountered in order of increasing depth. Asterisks next to electrode penetrations in the tonotopic area indicate correspondence between one of the threshold BFs and the BF of the composite tonotopic map. No multipeaked neurons were found in the small tonotopically organized reversal area (area C, Fig. 4). In 4 of the 5 penetrations with multiple multipeaked neurons in the tonotopic area, there is evidence for columnar organization of threshold BFs of multipeaked neurons.

formation must be processed in the cortex in parallel rather than sequentially.

The EFLs of delay-tuned neurons varied with location in the cortex. A composite cortical map of EFLs from eight bats corresponding to the delay-tuned neurons of Fig. 12 is illustrated in Fig. 17. Delay-tuned neurons in the variable area ($n = 48$) exhibited EFLs ranging from 5.6 to 16.8 ms with a mean of 10.2 ± 2.8 ms. In contrast, the spatial distribution of EFLs of delay-tuned neurons in the tonotopic area ($n = 36$) varied widely. EFLs ranged from 6.0 to 34.4 ms with a mean of 15.4 ± 7.4 ms. This range is long compared with the range of EFLs in the variable area. The difference in EFL between variable and tonotopic area delay-tuned neurons was significant (Systat, V 5.0, t test, $t = -4.473$, df = 82, $P < 0.000025$).

TABLE 2. *The columnar organization of multipeaked frequency-tuned neurons, BF_1 and BF_2 threshold frequencies in penetrations containing more than one neuron*

Bat	Neuron	BF_1, kHz	BF_2, kHz
E2290R	16-1	48.3	74.8
	16-3	19.4	65.2
E31090R	10-1	12	35
	10-2	10	30.5
E31390R	34-1	20	75
	34-2	20	75
	34-4	20	75
E5290R	16-3	16.5	32
	16-4	30	90
	18-2	23	69
	18-3	22	68
	18-4	21	67.5
	18-5	22	67.5
	32-1	22.5	65.5
	32-2	23.5	65
E51490R	28-2	17	60.5
	28-3	19.5	60

BF, best frequency.

Amplitude tuning of delay-tuned neurons

Cortical delay-tuned neurons are tuned to specific ranges of stimulus amplitudes in addition to echo delay. Both the pulse and the echo are part of the stimulus, and delay-tuned neurons exhibit maximum firing to particular values of pulse and echo amplitudes. These amplitudes are referred to as PBA and EBA. PBAs measured from delay-tuned neurons ($n = 99$) ranged from 51 to 103 dB SPL with an average of 78 ± 10 dB SPL. *Eptesicus* emits biosonar vocalizations at amplitudes of ~110 dB SPL in front of the bat (Kick and Simmons 1984), but the combination of middle ear and neural attenuation probably reduces the received amplitude by ~35–40 dB (Suga and Schlegel 1972; Suga and Shimozawa 1974) at the level of the cortex, which agrees with our pulse amplitude data.

Figure 18*A* shows a scatter plot of PBA against BD for each of the cortical delay-tuned neurons. The solid line represents the linear regression fit to the data, and the slope of the regression is 0.64 dB/ms, $r = 0.45$. This slope predicts an average decrease of almost 20 dB over a 30-ms range of BDs in the PBA tuning of the ensemble of delay-tuned neurons, but still with a considerable span of PBAs. To test whether this regression is representative of the population as opposed to a sampling bias, we computed the 99% confidence intervals on the regression line (Systat, V 5.0). The resulting slope of the lower confidence interval was positive and much greater than zero, demonstrating that the trend of decreasing PBAs with decreasing BDs is significant at $P < 0.01$. In contrast, PBAs measured in FM-FM area delay-tuned neurons in *Pteronotus* were systematically lower, averaging 64 ± 9 dB SPL with no trend of decreasing PBAs with decreasing BDs (Taniguchi et al. 1986).

EBAs measured from delay-tuned neurons ($n = 99$) in *Eptesicus* ranged from 36 to 86 dB SPL with an average of 57 ± 9 dB SPL. Figure 18*B* shows a scatter plot of EBAs versus BDs. The solid line represents the linear regression

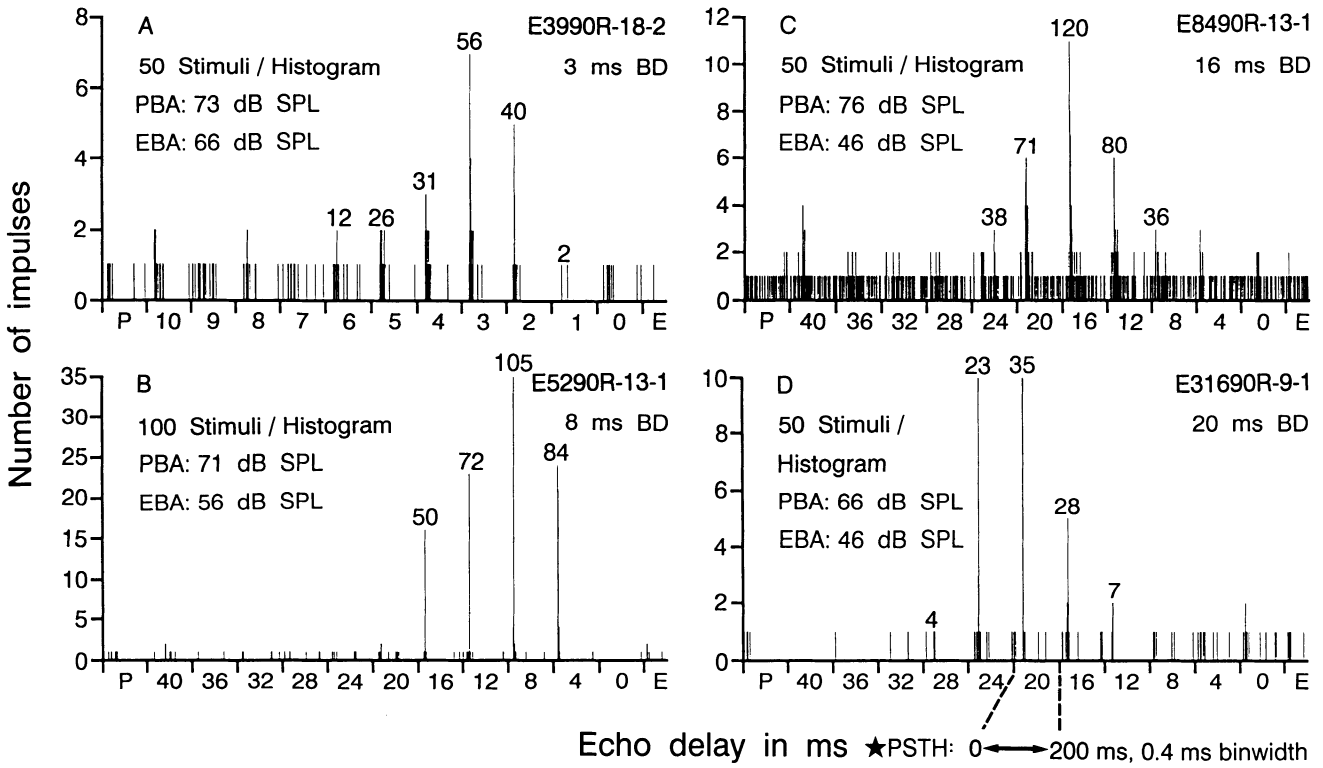

FIG. 10. *A–D*: responses of 4 delay-tuned cortical neurons. Each plot is a composite of multiple peristimulus time histograms (PSTHs) representing the neuronal responses to individual and paired FM stimuli simulating the biosonar vocalization (pulse) and returning echo. Each composite contains 13 PSTHs, with the 1st histogram for the pulse alone (P), then histograms for 10 pulse-echo pairs with different echo delays (*A*, 10–1 ms in 1-ms steps; *B–D*, 40–4 ms in 4-ms steps), then 1 histogram for simultaneous pulse and echo (0-ms echo delay), and finally 1 histogram for the echo alone (E). Segments defined by ticks on the horizontal axes (left to right) are individual 200-ms PSTHs with 0.4-ms binwidths at specific stimulus conditions as marked between the ticks. Numbers above peaks in the PSTHs indicate the total number of impulses elicited by the stimuli (pulse-echo pairs). Individual FM sounds were designed to mimic the biosonar signals and echoes of *Eptesicus*. Little neural response was evoked by a single pulse (P), a single echo (E), or the 0-ms pulse-echo pair. The maximum response was elicited by a combination of pulse and echo separated by a best echo delay (BD), and this response is greater than the sum of the individual pulse and echo responses. The maximum response also requires specific combinations of pulse and echo amplitudes, and these amplitudes are the best pulse amplitude (PBA) and best echo amplitude (EBA). As can be seen from the maximum number of impulses elicited by the pulse-echo pairs at BD, PBA, and EBA, delay-tuned neurons act as coincidence detectors that fire ~1 action potential per pulse-echo pair at BD.

fit to the data, and the slope of the regression is 0.40 dB/ms, $r = 0.30$. This slope predicts an average decrease of ~12 dB over a 30-ms range of BDs in the EBA tuning of the ensemble of delay-tuned neurons. We also computed the 99% confidence intervals on the EBA regression line (Systat, V 5.0). However, the resulting slope of the lower confidence interval was not different from zero, demonstrating that the trend of decreasing EBAs with decreasing BDs is not significant at $P < 0.01$. This result is similar to EBAs measured in FM-FM area delay-tuned neurons in *Pteronotus,* which averaged 56 ± 11 dB SPL with no trend of decreasing EBAs with decreasing BDs (Taniguchi et al. 1986), presumably because of the echo intensity compensation employed by this species (Gaioni et al. 1990; Kobler et al. 1985).

The difference in amplitude between the PBA and EBA for each of the delay-tuned neurons in *Eptesicus* ranged from 5 to 40 dB SPL with an average of 22 ± 7 dB SPL. Under natural conditions, echoes are lower in amplitude than vocalizations because of scattering and atmospheric attenuation (Griffin 1971; Lawrence and Simmons 1982), and the amplitude-tuning characteristics of delay-tuned neurons are consistent with this expectation.

Delay-tuned "amplitude shift" neurons

During the course of determining the delay-tuning properties of cortical neurons, it appeared that some delay-tuned neurons exhibited a change in BD with a change in pulse amplitude. The delay tuning of 25 neurons was evaluated with systematic changes in pulse amplitude, and 13 of these neurons clearly shifted their BD in response to changes in the pulse amplitude. These 13 delay-tuned neurons are referred to as *amplitude shift* neurons. The cortical location of 12 of the 13 amplitude shift neurons is illustrated by a superscript star to the right of the corresponding BD in Fig. 12. Seven of the 12 amplitude shift neurons are located in the variable area, and 5 of the 12 are in the tonotopic area. The proportion of amplitude shift neurons in each area to the total number is identical to the proportion of delay-tuned neurons in each area to the total number of delay-tuned neurons. This result, coupled with the composite distribution of amplitude shift neurons in the cortex (Fig. 12), suggests that amplitude shift neurons are randomly distributed among delay-tuned neurons.

The BDs associated with each amplitude shift cell (Fig. 12) represent the echo delay yielding the maximum facilitated response. However, the BD of amplitude shift cells is

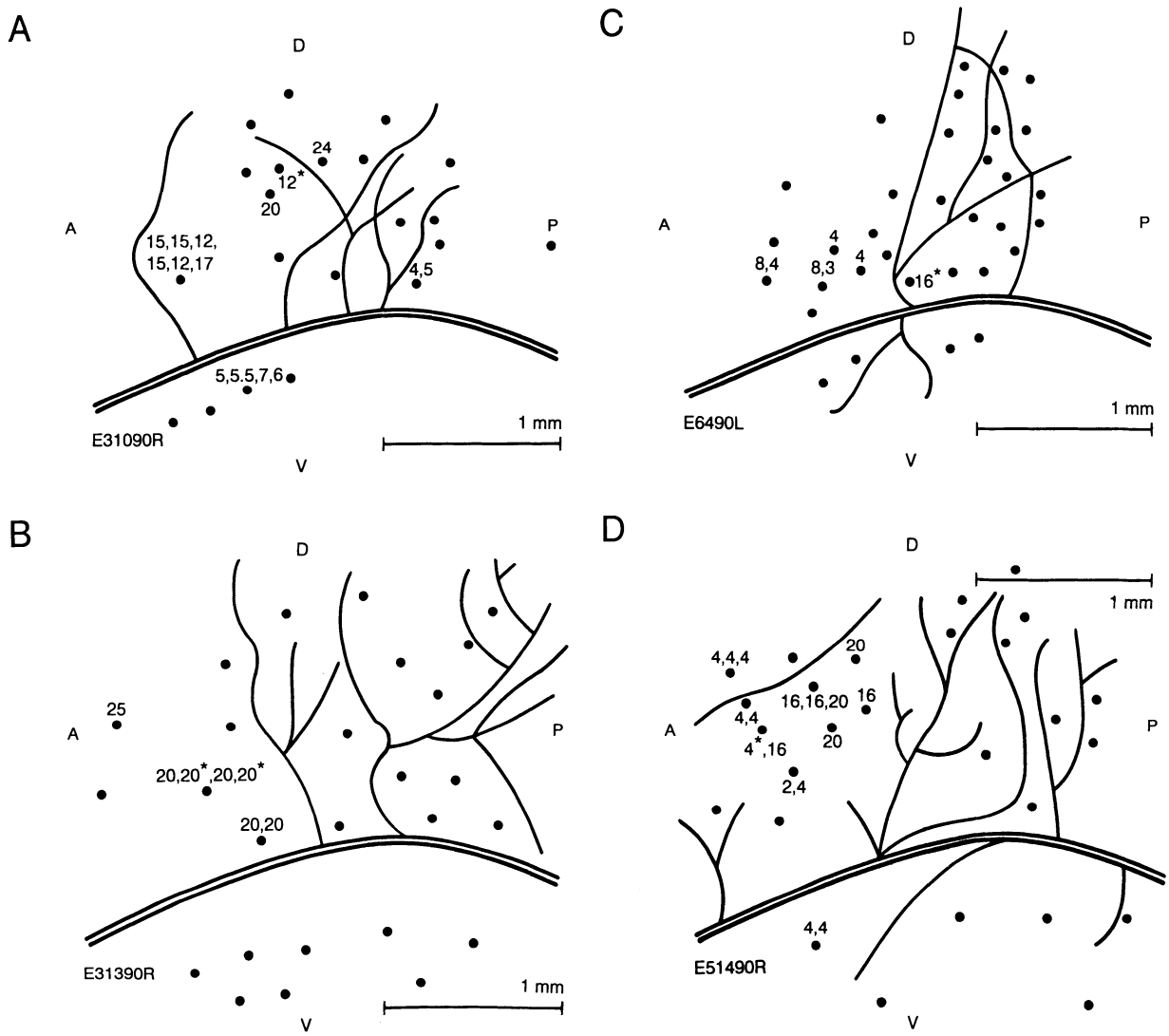

FIG. 11. Cortical maps from 4 individual bats illustrating the variability in the distribution of BDs of delay-tuned neurons. Circles without numbers represent electrode penetrations where no delay-tuned neurons were encountered. Numbers represent BDs in milliseconds. Electrode penetrations with multiple BDs separated by commas represent >1 delay-tuned neuron encountered in a single penetration and are presented in order of increasing depth. Starred numbers identify "amplitude shift" neurons (see text, Figs. 19 and 20), which comprise a subpopulation of delay-tuned neurons that change their BD in response to changes in pulse amplitude. BDs given for amplitude shift neurons are the BDs associated with their maximal neural response. Delay-tuned neurons do not appear to form a spatially distinct functional cortical subdivision.

capable of varying widely with pulse amplitude. The neural response of *amplitude shift neuron E5290R-12-4* to changes in pulse amplitude is illustrated in Fig. 19, *A–E*. This neuron exhibited a facilitated response to pulse amplitudes of 96–84 dB SPL with a fixed echo amplitude of 66 dB SPL. The pulse amplitude–induced shift in BD (star) from 24 to 8 ms can be seen in the sequence of delay-tuning curves as pulse amplitude was decreased from 89 to 85 dB SPL in 1-dB steps.

The ensemble of amplitude shift neurons responds to a wide range of pulse amplitudes with a wide range of echo delays. The response of *amplitude shift E5290R-15-1* shown in Fig. 20*A* is an example. Each circle represents a combination of pulse amplitude and the associated BD, and the neural response can be separated into three phases (1, 2, and 3) with arrows marking the boundaries between phases. The first neural response phase starts at high pulse amplitude. The BD decreased from 36 to 32 ms and then remained constant at 32 ms for decreasing pulse amplitudes of 94–90 dB SPL. The second neural response phase is characterized by a linear decrease of BD with decreasing pulse amplitudes from 90 to 80 dB SPL. In the third neural response phase the BD remained constant at 4 ms for pulse amplitudes <80 dB SPL. Neural firing rate was highest during the second neural response phase.

A summary of changes in BD in response to changes in pulse amplitude for all amplitude shift neurons appears in Fig. 20*B*. Each solid line represents data from a single shift neuron with upper and lower endpoints (●) marking the range of BD change at different PBAs during the second response phase. There is little similarity among slopes of the lines connecting the endpoints for the amplitude shift neurons. Of the 13 amplitude shift neurons, 11 exhibited a *decrease* in BD in response to a *decrease* in pulse ampli-

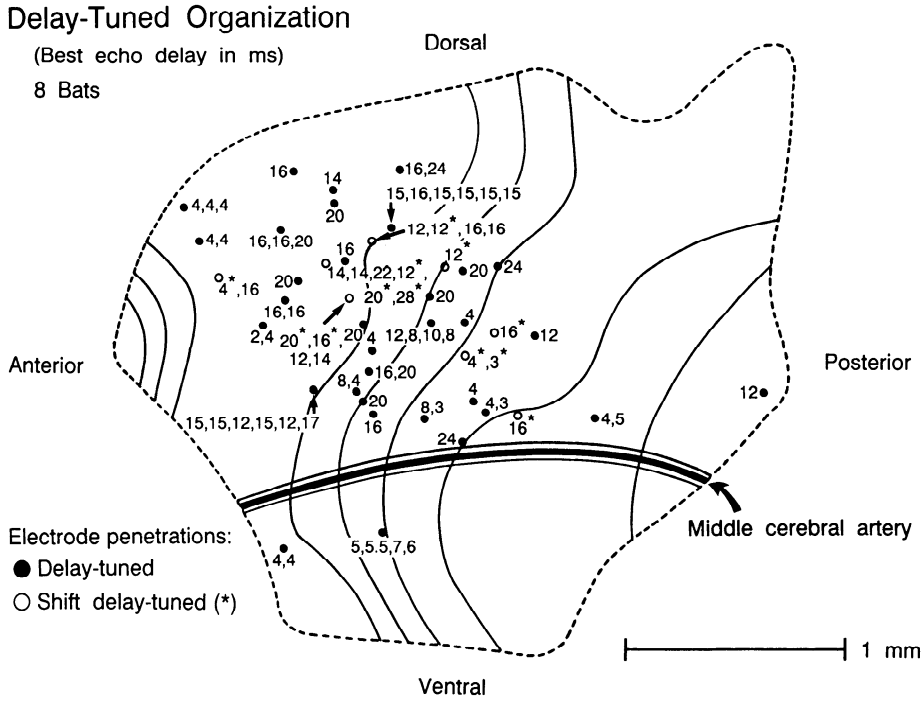

FIG. 12. Composite spatial representation of BD of delay-tuned neurons (n = 84) from the auditory cortices of 8 bats superimposed on the isofrequency contours of the composite tonotopic map (see Fig. 4). Symbols (○ and ●) represent electrode penetrations containing only delay-tuned neurons (●) or both delay-tuned neurons and amplitude shift cells (○). Numbers represent the BD in milliseconds. Multiple numbers separated by commas represent the BDs of sequential delay-tuned neurons encountered in a single penetration in order of increasing depth. Delay-tuned neurons were found in the variable area (n = 48) and the high-frequency portion of the tonotopic area (n = 36). There is the suggestion of delay-tuned axis in the anterior region of the cortex corresponding to the variable area (see Fig. 4), but all the short BD (2–4 ms) neurons come from one bat, *E51490R* (see Fig. 11*D*). The global organization of delay tuning is not topographic.

tude, and 2 neurons *increased* their BD in response to *decreasing* pulse amplitude.

Pulse amplitudes at the boundary between the first and second response phases for amplitude shift neurons (n = 13) ranged from 76 to 103 dB SPL with an average of 87 ± 8 dB SPL. Pulse amplitudes at the boundary between the second and third response phases ranged from 56 to 91 dB SPL with an average of 75 ± 12 dB SPL. The difference between pulse amplitudes at the response phase boundaries for each of the amplitude shift neurons ranged from 3 to 30 dB SPL with an average of 13 ± 8 dB SPL.

BDs at the boundary between the first and second response phases for amplitude shift neurons (n = 13) ranged from 5 to 32 ms with an average of 18 ± 8 ms. BDs at the boundary between the second and third response phases ranged from 2 to 20 ms with an average of 10 ± 7 ms. The difference between BDs at the response phase boundaries for each of the amplitude shift neurons ranged from 3 to 28 ms with an average of 11 ± 8 ms.

DISCUSSION

Nontopographic global distribution of cortical delay-tuned neurons

Cortical delay-tuned neurons reported in this study are tuned to particular values of echo delay in similar fashion to

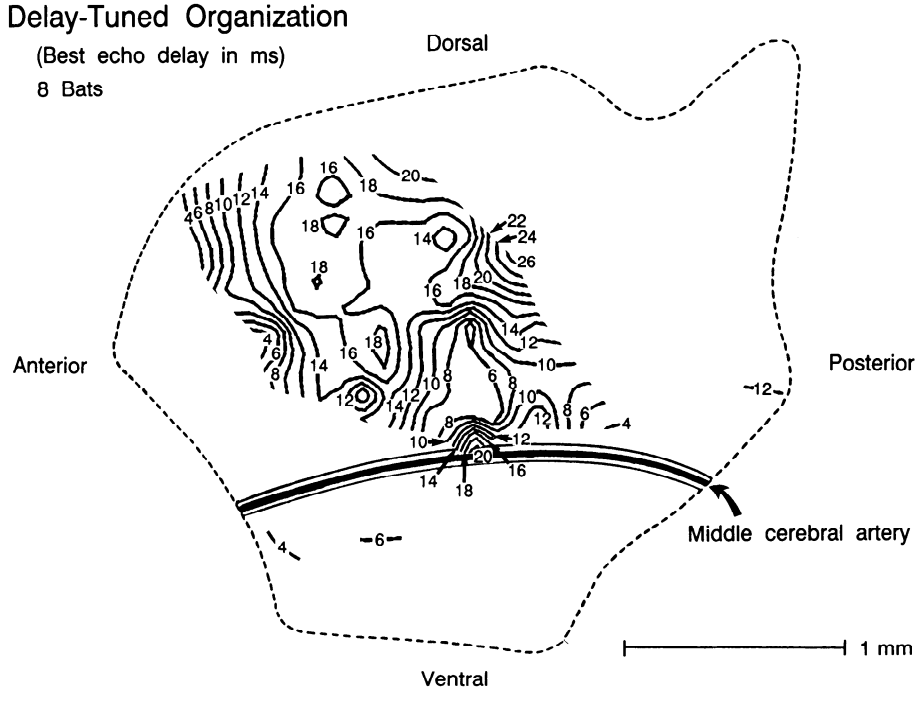

FIG. 13. Computer-generated BD contour map representing the BD cortical composite map data (Fig. 12). Lines on the cortical surface represent BD contours in echo delay steps of 2 ms. Because a contour plot represents the spatial distribution of BDs in an unbiased fashion, systematic cortical organization of BDs should appear as a series of parallel lines perpendicular to a BD axis. The pattern of contour BD lines does not represent a pattern of systematic global BD organization, linear, radial, or otherwise.

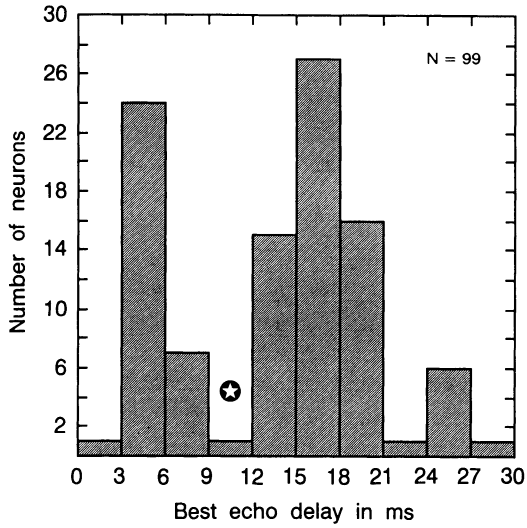

FIG. 14. Histogram representing the distribution of cortical BDs of delay-tuned neurons (n = 99). BDs range from 2 to 28 ms (corresponding to target ranges of 35–485 cm). Star identifies a gap in the distribution from 6 to 15 ms, even though echo-delay values in this region were sampled. These data suggest that the distribution of cortical BDs is bimodal.

cortical delay-tuned neurons in other species of echolocating bats (Berkowitz and Suga 1989; O'Neill and Suga 1979, 1982; Schuller et al. 1989, 1991; Shannon-Hartman et al. 1992; Suga and O'Neill 1979; Suga et al. 1978; Sullivan 1982; Wong and Shannon 1988). One result in the response properties of cortical delay-tuned neurons in *Eptesicus* that is strikingly different is the average of about one action potential per pulse-echo pair as compared with the multiple action potentials generated by cortical delay-tuned neurons in *Pteronotus* (Suga and Horikawa 1986; Suga et al. 1983). This result raises the possibility of further temporal organization of cortical delay-tuned neurons in *Eptesicus.*

Another interesting result is the bimodal distribution of cortical BDs in *Eptesicus.* The distribution of cortical BDs in *Myotis* also appears bimodal, but the gap between the modes spans BDs of 3–5 ms (Sullivan 1982). In *Eptesicus* the distribution of BDs in the first mode (2–10 ms) appears similar to the single mode distribution of cortical BDs measured in the FM-FM area of *Pteronotus* (Suga and Horikawa 1986) and *Rhinolophus* (Schuller et al. 1991). Although *Pteronotus* and *Rhinolophus* exhibit cortical neurons with BDs >10 ms, the incidence of neurons with these BDs is rare. In contrast, there are many neurons with BDs in the 10- to 28-ms range in *Eptesicus,* suggesting a considerably longer working range for echolocation in this species.

The principal new finding of our study is that BDs of cortical delay-tuned neurons in *Eptesicus* are not systematically arrayed across the cortex to form a global topographic axis of echo delay or target range. Our result is very similar to the organization of cortical delay tuning observed in *Myotis.* The distribution of delay-tuned neurons in *Myotis* encompasses a large cortical field, containing both delay-tuned and non–delay-tuned neurons (Shannon-Hartman et al. 1992; Wong and Shannon 1988). Furthermore, there is no clear systematic, global, topographic organization of BD across the cortical surface in *Myotis* (Wong and Shannon 1988).

Our result is in contrast to the topographic axes of echo delay observed in *Pteronotus* and *Rhinolophus* cortex. Delay-tuned neurons in *Pteronotus* cluster into three separate cortical fields: the FM-FM area, DF, and VF (Edamatsu et al. 1989; O'Neill and Suga 1979, 1982; Suga and Horikawa 1986; Suga and O'Neill 1979; Suga et al. 1978, 1983b). BDs of delay-tuned neurons are arrayed in a gradient oriented along the anteroposterior axis of each field, yielding multiple cortical representations. The composition of neuronal response types in the fields is mostly homogeneous, containing delay-tuned neurons. Differences in neuronal response properties between the fields include the span of BDs encompassed by each area and the EFLs.

Delay-tuned neurons in *Rhinolophus* cortex cluster in a single field, with a gradient in the BD of neurons oriented along the anteroposterior axis of the field (Schuller et al. 1991). Interestingly, the topographic gradient of BDs in *Rhinolophus* contains a linear region, corresponding to an overrepresentation of neurons with BDs around 3 ms BD. Unlike *Pteronotus,* however, the composition of the delay-tuned field is not homogeneous, containing both delay-tuned neurons and non–delay-tuned neurons. There is no evidence for multiple representations for delay-tuned axes in *Rhinolophus* as there is in *Pteronotus* (Schuller et al. 1991; Suga and Horikawa 1986).

The demonstration of topographic axes of echo delay in *Pteronotus* and *Rhinolophus* relied on the methodology of oblique electrode penetrations, whereas the results from *Myotis* and from our study employed the methodology of orthogonal penetrations and required pooling of BD data from many individual bats. The difference in data collection methodologies between studies offers one possible hypothesis concerning the difference in cortical organization of delay tuning between *Eptesicus, Myotis,* and other species. The hypothesis is that delay tuning is actually topographically organized in *Eptesicus,* and the observed nontopographic organization of delay tuning results from arti-

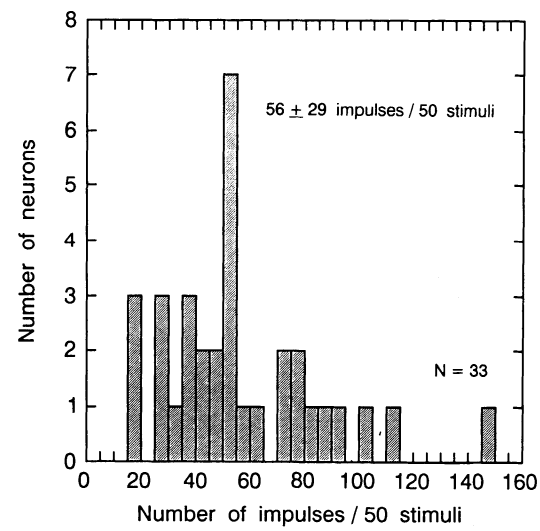

FIG. 15. Histogram representing the distribution of the number of impulses from single-unit recordings of delay-tuned neurons evoked by 50 pulse-echo pairs. Pulse amplitudes, echo amplitudes, and echo delays were adjusted for each neuron to elicit the maximum number of impulses. The 33 neurons responded with an average of 56 ± 29 imp/50 pairs, ~1 action potential per stimulus pair.

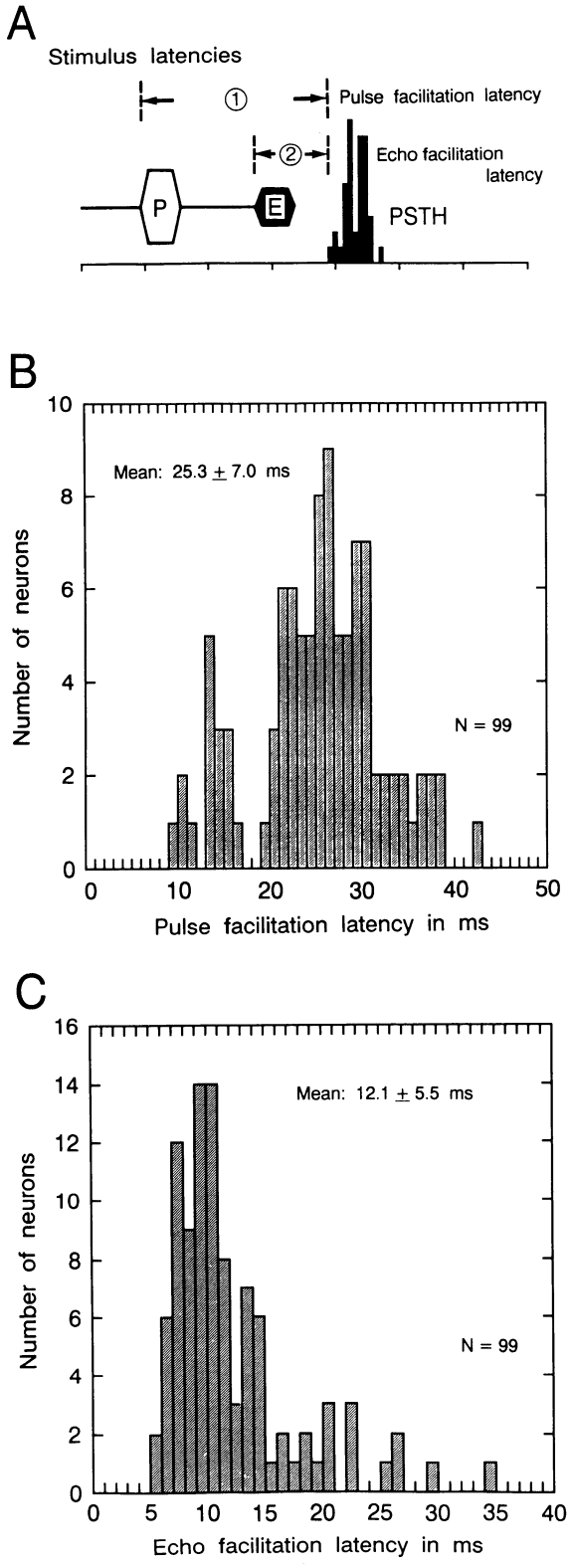

FIG. 16. *A*: delay-tuned neuron responds to the reception of an echo after a specific time interval after vocalization by firing an action potential, and the response latency of a delay-tuned neuron to the stimulus pair can be characterized with respect to the simulated vocalization or pulse (P) as the *pulse facilitation latency* (PFL, 1) or with respect to the echo (E) as the *echo facilitation latency* (EFL, 2). *B*: histogram representing the distribution of PFLs of cortical delay-tuned neurons ($n = 99$). PFLs ranged from 9.1 to 42.4 ms, with a mean of 25.3 ± 7.2 ms. *C*: histogram representing the distribution of EFLs for cortical delay-tuned neurons ($n = 99$). EFLs ranged from 5.6 to 34.4 ms, with a mean of 12.1 ± 5.5 ms.

facts introduced by the pooling of BD data across individual topographically organized bats. Our results provide three lines of evidence against this hypothesis.

The first line of evidence against the global topographic organization of BD hypothesis draws on the comparison of the distribution of BDs (Fig. 12) and EFLs (Fig. 17) between variable area and tonotopic area delay-tuned neurons. If the topographic hypothesis were correct, by implication all neurons should have a similar distribution of response properties because only the action of pooling would have caused relative displacement of delay-tuned neurons in the composite map. We tested this hypothesis by comparing the EFLs of delay-tuned neurons with BDs of 3–5 ms located in the 20- to 30-kHz and 30- to 40-kHz regions of the tonotopic area ($n = 8$, Figs. 12 and 17) with EFLs of 2- to 5-ms BD neurons in the variable area ($n = 8$, Figs. 12 and 17). EFLs for the subset of tonotopic area delay-tuned neurons ranged from 9.2 to 34.4 ms with an average 21.9 ± 9.2 ms as compared with a range of 6.0–12.0 ms with an average of 8.9 ± 2.7 ms for the subset of variable area delay-tuned neurons. The difference in EFLs was significant (Systat, V 5.0, *t* test, $t = -3.895$, df = 14, $P < 0.002$). Thus, on the basis of the difference in distribution of EFLs, it is unlikely that tonotopic area delay-tuned neurons with BDs of 3–5 ms are variable area delay-tuned neurons displaced by pooling.

The second line of evidence against a global topographic cortical organization of BD is the presence of amplitude shift cells that change BD in response to shifts in pulse amplitude. There is a correspondence between pulse amplitudes of 87–75 dB SPL eliciting large shifts in BD for amplitude shift neurons and the average best pulse amplitude of 78 ± 10 dB SPL for all delay-tuned neurons. There is an additional correspondence between the average change in pulse amplitude of 13 ± 8 dB for amplitude shift neurons and the average decrease by 10–15 dB in the vocalization amplitude at the beginning of the terminal stage of insect pursuit (Jen and Kamada 1982; Kick and Simmons 1984). Together these correspondences suggest that amplitude shift neurons are activated during normal insect pursuit behavior and that their shifting delay tuning is functionally important. Some amplitude shift cells can shift their BDs by up to 28 ms (Fig. 20*A*). This result, coupled with the nonuniform rate of BD change with pulse amplitude change (Fig. 20*B*) is incompatible with a global topographic organization of BD that had been missed because of the use of pooled data.

Cortical delay-tuned neurons that exhibit different BDs in response to either changing stimulus amplitudes or repetition rates have previously been described in *Pteronotus* (O'Neill and Suga 1982; Suga et al. 1978; Taniguchi et al. 1986) and *Myotis* (Sullivan 1982; Teng and Wong 1992; Wong et al. 1992). "Tracking neurons" in the FM-FM area of *Pteronotus* exhibit a decrease in BD with increasing stimulus pair repetition rate (O'Neill and Suga 1982; Suga et al. 1978). Although not suitable for target ranging, presumably, the reduction in BD occurs continuously during insect pursuit in response to the continuous increased rate of emitted sounds, allowing the neurons to track the target's closing range. This result is different from amplitude shift cells in *Eptesicus*, where the shift in BD presumably occurs

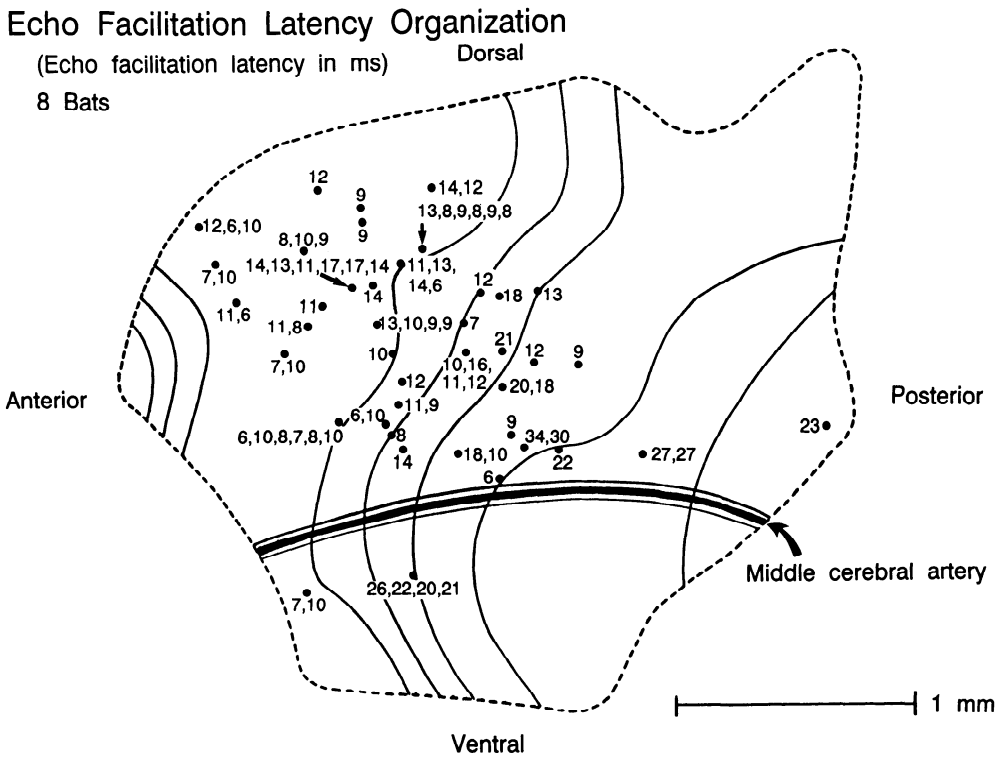

FIG. 17. Composite spatial representation of EFLs of delay-tuned neurons (n = 84) from the auditory cortices of 8 bats superimposed on the isofrequency contours of the composite tonotopic map (Fig. 4). Circles represent electrode penetrations containing delay-tuned neurons (Fig. 12), and numbers represent the EFL in ms. Multiple numbers separated by commas represent the EFLs of sequential delay-tuned neurons encountered in a single penetration in order of increasing depth. EFLs of neurons in the variable area (n = 48) exhibited EFLs ranging from 5.6 to 16.8 ms with a mean of 10.2 ± 2.8 ms. EFLs of neurons in the tonotopic area (n = 36) ranged from 6.0 to 34.4 ms with a mean of 15.4 ± 7.4 ms. The difference between these two distributions is statistically significant.

at the beginning of the terminal stage of insect pursuit. The delay-tuning curves of tracking neurons are typically "U shaped" for low repetition rates (10/s) and shift to a shorter BD and become more "V shaped" at higher repetition rates (100/s). BD shifts appear to range from 2 to 4 ms BD, so the overall change in BD is small compared with changes in

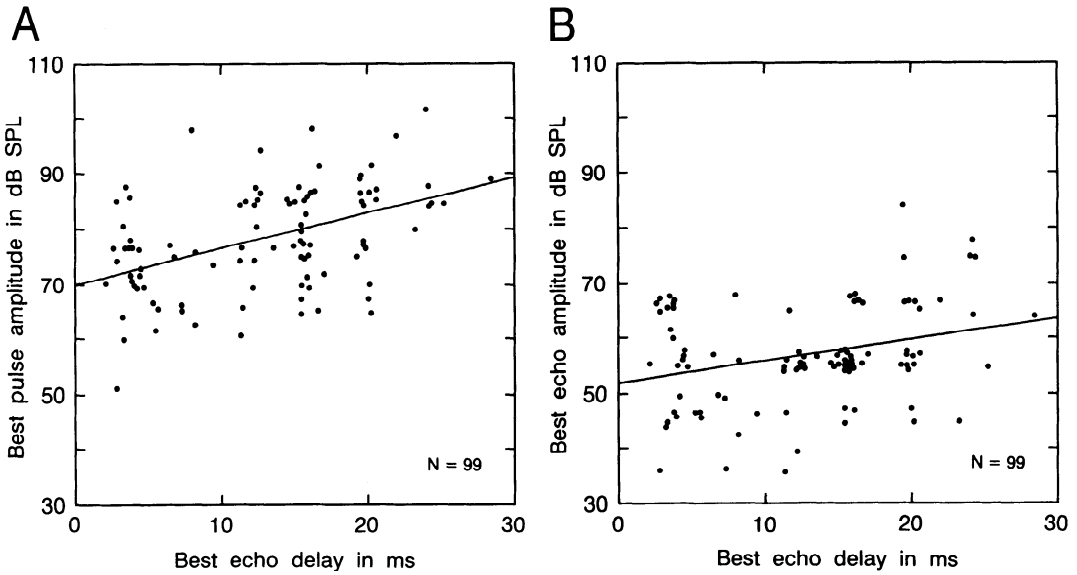

FIG. 18. *A*: scatter plot of PBA vs. BD of cortical delay-tuned neurons. Solid line represents a linear regression fit to the data, which is significantly different from a horizontal line based on the 99% confidence intervals to the regression fit. The decreasing trend in PBA may be related to pulse intensity compensation during approach to the target (see text). *B*: scatter plot of EBA vs. BD. Echoes are typically weaker than vocalizations at the bat's ears, and the range of EBAs is less than the range of PBAs. Solid line represents a linear regression fit to the data, which is not significantly different from a horizontal line based on the 99% confidence intervals to the regression fit.

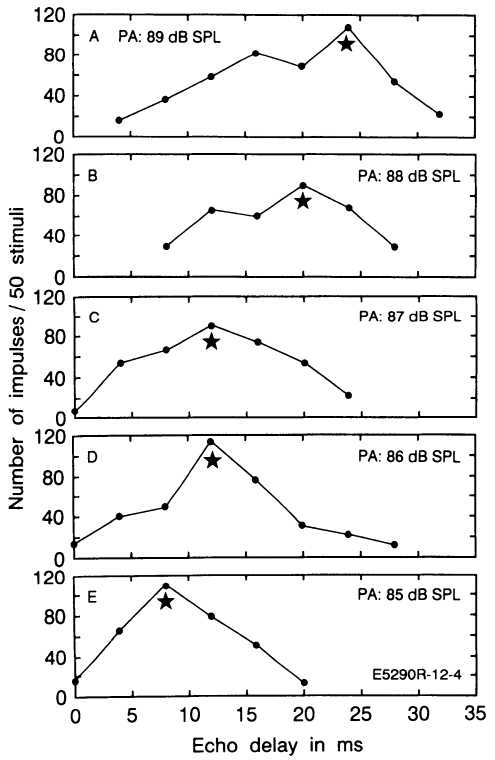

FIG. 19. Typical cortical "amplitude shift" neuron. *A–E*: sequence of delay-tuning curves recorded from an amplitude shift neuron elicited by 50 pulse-echo pair stimulus presentations at different echo delays. Stars mark the BD of each delay-tuning curve. Pulse amplitudes associated with each delay-tuning curve are indicated on each plot, and the echo amplitude was fixed at 66 dB SPL for all the delay-tuning curves. A systematic decrease in BD from 24 to 4 ms can be observed as the pulse amplitude is decreased.

BD of amplitude shift cells in *Eptesicus*. The shift to shorter BDs of tracking neurons in response to higher repetition rates appears to be accomplished through progressive suppression of echo delays greater than BD, resulting in a progressively narrower delay-tuning curve. Delay-tuning curves of amplitude shift cells in *Eptesicus* are "V shaped" and do not systematically change in width with progressive changes in BD (Fig. 19).

The effect of changing pulse amplitude was studied also with FM-FM area neurons in *Pteronotus* (Taniguchi et al. 1986). About one-third of delay-tuned neurons tested exhibited a decrease in BD in response to a decrease in pulse amplitude. However, the change in BD was very small. Taken together, all the preceding results suggest that the functional roles and mechanisms creating delay-tuned neurons with variable BD are different in *Eptesicus* and *Pteronotus*.

Myotis, like *Eptesicus*, does not appear to exhibit global topographic organization of cortical BD (Wong and Shannon 1988). About 22% of cortical delay-tuned in *Myotis* are tracking neurons that exhibit an average decrease of 5.7 ± 2.6 ms for an increase in pulse repetition rate (Wong et al. 1992). The shift to shorter BDs of tracking neurons in response to higher repetition rates appears to be accomplished through a progressive shift in the delay-tuning curve (Wong et al. 1992), unlike tracking neurons in *Pteronotus* (O'Neill and Suga 1982; Suga et al. 1978). *Myotis* cortex also contains amplitude shift neurons (Sullivan 1982; Teng and Wong 1992). About 25% of amplitude shift neurons systematically shift their BD in response to pulse amplitudes (Teng and Wong 1992) and exhibit changes in BD of up to 5 ms (Sullivan 1982). The changes in BD of tracking neurons and amplitude shift neurons in *Myotis* are large compared with the maximum BD of 18 ms (Wong et al. 1992).

We did not vary the repetition rate of the stimulus pair in our study, so we cannot report on the presence of repetition rate-tuned or tracking neurons in *Eptesicus*. The potential presence of these types of delay-tuned neurons could increase the relative number of cortical delay-tuned neurons but are not likely to improve the cortical organization of BD.

It is interesting to note that the CF-FM bats *Pteronotus* and *Rhinolophus* both exhibit systematic topographic organization of cortical BD (Edamatsu et al. 1989; O'Neill and Suga 1979, 1982; Schuller et al. 1991; Suga and Horikawa 1986; Suga and O'Neill 1979; Suga et al. 1978, 1983) and that cortical tracking or amplitude shift neurons in *Pteronotus* are either rare or change little (O'Neill and Suga 1982; Suga et al. 1978; Taniguchi et al. 1986). In contrast, the FM bats *Eptesicus* and *Myotis* do not appear to exhibit global systematic topographic organization of cortical BD (Wong and Shannon 1988), and both contain significant numbers of delay-tuned neurons with BDs that change in response to changes in pulse amplitude (Sullivan 1982). In addition, *Myotis* contains significant numbers of delay-tuned neurons with BDs that change in response to repetition rate and echo duration (Teng and Wong 1992; Wong et al. 1992). All these results raise the interesting possibility that CF-FM and FM bats represent and process cortical range information in different ways.

The third line of evidence against a global topographic cortical organization of BD is the lack of consistent columnar organization of BD in electrode penetrations containing amplitude shift delay-tuned neurons. Our protocol did not include histological verification of recording electrode penetrations, so the orthogonality of the penetrations could not be verified anatomically. However, the majority of our BF data was organized in columns in similar fashion to other studies in awake animals (Abeles and Goldstein 1970; Evans and Whitfield 1964; Evans et al. 1965; Galambos 1960; Suga and Manabe 1982). In addition, columnar organization was also observed in five out of seven orthogonal penetrations containing multipeaked frequency-tuned neurons (Table 2). Yet, under *identical* recording conditions during the *same* recording sessions, BDs of cortical delay-tuned neurons recorded sequentially in orthogonal penetrations were more variable. Of the 21 electrode penetrations (Fig. 12) containing 2 or more sequentially recorded delay-tuned neurons, 11 penetrations exhibited neurons that differed in BD by ≥4 ms. Thus about one-half of the electrode penetrations did not exhibit columnar organization of BD. Almost ½ of the 11 noncolumnar penetrations contained amplitude shift cells. Thus the appearance of noncolumnar delay-tuned organization may, in part, be due to amplitude shift cells. In contrast, BDs of cortical delay-tuned neurons in *Pteronotus* are organized in columns (Suga and O'Neill 1979). However, cortical delay-

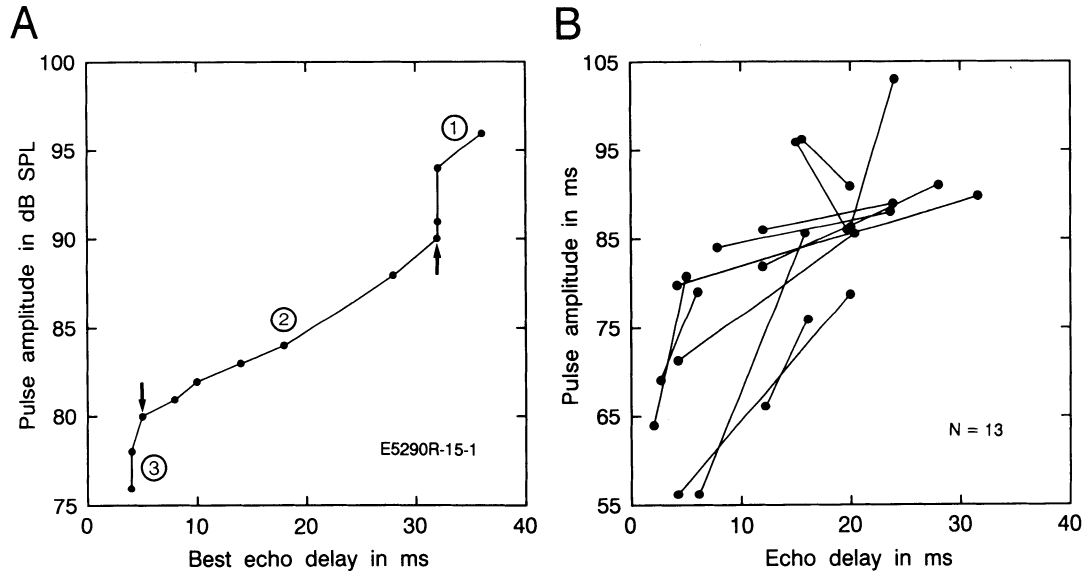

FIG. 20. *A*: BDs as a function of pulse amplitude for an amplitude shift neuron. Each filled circle represents a combination of pulse amplitude and its associated BD. Circled numbers represent the typical neural response phases to changes in pulse amplitude, and arrows mark boundaries between neural response phases. In neural response phase 1, the BD decreases from 36 to 32 ms and remains constant at 32 ms for pulse amplitudes of 94–90 dB SPL. In the 2nd neural response phase for pulse amplitudes between 90 and 80 dB SPL, the BDs decrease as a linear function of pulse amplitude. In the 3rd neural response phase for pulse amplitudes <80 dB SPL, the BD remains constant around 4 ms. *B*: summary of cortical shift neurons exhibiting changes in BD in response to changes in pulse amplitude. Each solid line represents data from a single shift neuron with upper and lower endpoints marking the range of BD at different PBAs. *Eptesicus* lowers its vocalization amplitude during the final ½ m of insect pursuit until interception (see text), and most cortical shift neurons are expected to respond with decreasing BDs to decreasing pulse amplitude. The range of BDs spanned by cortical shift neurons completely overlaps the range of BDs associated with nonshifting delay-tuned neurons, and the slopes of the shift lines are different.

tuned neurons in *Rhinolophus* appear to be limited to cortical layer 5 with little variation of BDs in orthogonal penetrations (Schuller et al. 1991).

Potential local organization of delay-tuned neurons

The significant differences in distribution of BD and EFL data from variable and tonotopic area delay-tuned neurons in *Eptesicus* suggest an alternative hypothesis that cortical delay-tuned neurons in the variable and tonotopic areas are multiple representations of target range. The difference in the distribution of EFLs in the variable and tonotopic areas of *Eptesicus* cortex is similar to the difference in the distribution of EFLs in FM-FM and DF areas of *Pteronotus* cortex. The average EFL of the variable area delay-tuned neurons is 10.2 ± 2.8 ms as compared with an average EFL of 15.4 ± 7.4 ms in the tonotopic area delay-tuned neurons. The average EFL of the FM-FM area delay-tuned neurons is 8.8 ± 2.1 ms as compared with an average EFL of 15.2 ± 7.2 ms for DF area delay-tuned neurons (Suga and Horikawa 1986).

The distributions of cortical BDs in *Eptesicus* are different from the distributions of cortical BDs in *Pteronotus*. Delay-tuned neurons in both the variable and tonotopic areas typically exhibit BDs of ≥24 ms. However, the average BD is 14.4 ± 5.4 ms for variable area neurons as compared with an average BD of 9.9 ± 6.6 ms for tonotopic area neurons. In the FM-FM area, BDs typically range to 18 ms as compared with 9 ms for the DF area even though both areas share the same average BD of 3.5 ms (Suga and Horikawa 1986). In summary, the significantly different distributions of EFL, coupled with the combination of significantly different distributions of BDs suggest that the delay-tuned neurons in the variable and tonotopic areas constitute multiple cortical representation of target range in *Eptesicus*.

Although global topographic organization of BD in *Eptesicus* cortex is unlikely, our results suggest the possibility of local topographic organization of BD. The delay-tuned neurons of *bat E51490R* (Fig. 11*D*) that are located in the variable area form an axis of BD oriented anterior to posterior, if the presence of amplitude shift cells is ignored. The organization of BDs of variable area delay-tuned neurons from other bats included in the composite map (Fig. 12), although lacking short BDs, are consistent with this axis of BD (Figs. 12 and 13). Because the representation of BD in the tonotopic area is not topographically organized on the same scale as the tonotopic representation of BF, it seems unlikely that BD in the tonotopic area is topographically organized.

The location and orientation of BDs in the variable area are similar to the location and orientation of delay-tuned neurons in *Rhinolophus* cortex and FM-FM area delay-tuned neurons in *Pteronotus* (O'Neill and Suga 1979, 1982; Schuller et al. 1991; Suga and O'Neill 1979; Suga et al. 1978, 1983). Furthermore, the average EFL of variable area delay-tuned neurons is 10.2 ± 2.8 ms, which is similar to the average EFL of 8.8 ± 2.1 ms of FM-FM area delay-tuned neurons in *Pteronotus* (Suga and Horikawa 1986) and of 8.3 ± 0.8 ms of cortical delay-tuned neurons in *Myotis* (Sullivan 1982). Together, these results suggest that variable area delay-tuned neurons in *Eptesicus* may be analogous to the FM-FM area in *Pteronotus*.

Functional interpretation of multipeaked frequency-tuned neurons

In this section we consider a potential functional role for neurons with multipeaked frequency-tuning curves. No multipeaked neurons were found in a previous study of the frequency organization of *Eptesicus* cortex (Jen et al. 1989). In contrast to the previous study, our results demonstrate multipeaked neurons and auditory responses situated ventral to the middle cerebral artery. One possible explanation for these differences in results is the potential effects from anesthesia used during recording sessions in the previous study, whereas our recordings were made in awake bats.

The finding that the majority of these multipeaked neurons exhibit threshold BF ratios of about three-to-one suggests their involvement in the parallel, distributed process of encoding of target range information via spectral interference in echoes. Real targets such as moths contain multiple reflective surfaces at different ranges, and echoes returning from these targets contain interference peaks and notches in their spectra (Beuter 1980; Habersetzer and Vogler 1983; Kober and Schnitzler 1990; Simmons and Chen 1989). Behavioral experiments have shown that *spectral notches alone* are a sufficient biosonar cue for the discrimination of complex targets and the perception of multiple target ranges (Habersetzer and Vogler 1983; Mogdans and Schnitzler 1990; Schmidt 1988, 1992; Simmons et al. 1990).

Spectral notches are caused by interference due to cancellations at specific frequencies. They appear at regular frequency intervals, the value of the interval being determined by the arrival-time differences among echoes returning from the multiple reflective surfaces. Figure 21*A* illustrates waveforms of three different multiple echoes of the same *Eptesicus* biosonar signal reflected from two surfaces separated by different ranges of 0, 9, or 18 mm, corresponding to time delay differences of 0, 50, or 100 μs. As the separation time between echoes increases, the envelope of the signal contains more rapid modulations as spectral notches shift closer together. In particular, interference causes the cancellation of frequencies (F) depending on the separation time (T_{sep}) between glints related by *Eq 1*.

$$F = (2n + 1)/T_{sep} \quad n = 0, 1, 2, \cdots \qquad (1)$$

Thus interference causes spectral notches with different orders (n) in returning echoes at odd harmonically related frequencies (1, 3, 5, $\cdots$). Both the number and spacing of notches depends on the separation time of the echoes. Figure 21*B* shows the family of hyperbolic curves that define spectral notches at the 1st through 10th orders as a function of the separation time of two glints and the frequency of the spectral notches caused by the interference. Separation distance (relative range) between the glints is linearly related to the separation time between the glints by 5.8 μs/mm of range difference. From the placement of the curves in Fig. 21*B*, transformation of spectral notches back to estimates of time or distance separation may be accomplished most effectively by the use of only the first- or third-order notch frequencies when multiple spectral notches are present.

Multipeaked frequency-tuned neurons with their odd harmonic BF ratios of three-to-one offer a possible means of encoding spectral notches. The results of a recent computational model with parallel pathways for processing temporal and spectral information contained in echoes demonstrates successful reconstruction of target shape by the use of echo delay and spectral notches to reconstruct a unified representation of target range (Saillant et al. 1993; Simmons et al. 1992). The performance of the model accurately reproduces the images perceived by *Eptesicus* as measured in a variety of behavioral experiments on two-glint resolution in range, echo phase sensitivity, amplitude-latency trading of range estimates, dissociation of time and frequency domain image components, and fine ranging accuracy in noise. The spectral-notch computational pathway relies on signal processing elements that can be synthesized by an *ensemble* of multipeaked frequency-tuned neurons. An ensemble of multipeaked frequency-tuned neurons is necessary to unambiguously decode spectral interference patterns, because two-glint targets with echo separation times $\geq$25 ms generate more than two spectral notches (Fig. 21*B*). For three-glint targets, the decoding process becomes more complex.

The critical test of the hypothesis that multipeaked frequency-tuned neurons encode spectral notches to estimate echo-delay separation is that the neural response of multipeaked frequency-tuned neurons should be different for synthesized biosonar echoes with and without notches. The responses of multipeaked frequency-tuned neurons to individual tone bursts predict a *lower* firing rate for echoes (FM sweeps) containing spectral notches as compared with the response to unnotched echoes (FM sweeps). This predicted response appears unusual in the following respect. Typical neurons encoding information-bearing parameters (Suga 1984) are expected to discharge *only* in response to specific features of biologically relevant stimuli. Multipeaked frequency-tuned neurons are predicted to exhibit a response to all echoes. The magnitude of the response is expected to depend on the spectral content of the echoes, and biologically relevant stimuli, spectral notches, are expected to *decrease* the maximum response.

Finally, of the 653 auditory neurons recorded in this study, only 99 or $\sim$15% were delay tuned. In contrast, delay-tuned neurons in *Rhinolophus* comprised 44% of the cortical population of auditory neurons (Schuller et al. 1991). Delay-tuned neurons in *Pteronotus* form three cortical subdivisions (Edamatsu et al. 1989; O'Neill and Suga 1979, 1982; Suga and Horikawa 1986; Suga and O'Neill 1979; Suga et al. 1978, 1983). Delay-tuned neurons, tracking neurons, and amplitude shift cells comprise 77% of the neurons in the auditory cortex of *Myotis* (Sullivan 1982; Wong et al. 1992). If an ensemble of cortical multipeaked frequency-tuned neurons could encode fine-range separations, then this result may help explain the relative scarcity of cortical delay-tuned neurons in *Eptesicus*. Also, delay-tuned neurons tuned to stimulus repetition rates not used in our study may also increase the relative number of cortical delay-tuned neurons.

Functional interpretation of overlapping cortical fields

Information about the fine-range structure of a target is carried by spectral notches in echoes (Beuter 1980; Habersetzer and Vogler 1983; Mogdans and Schnitzler 1990;

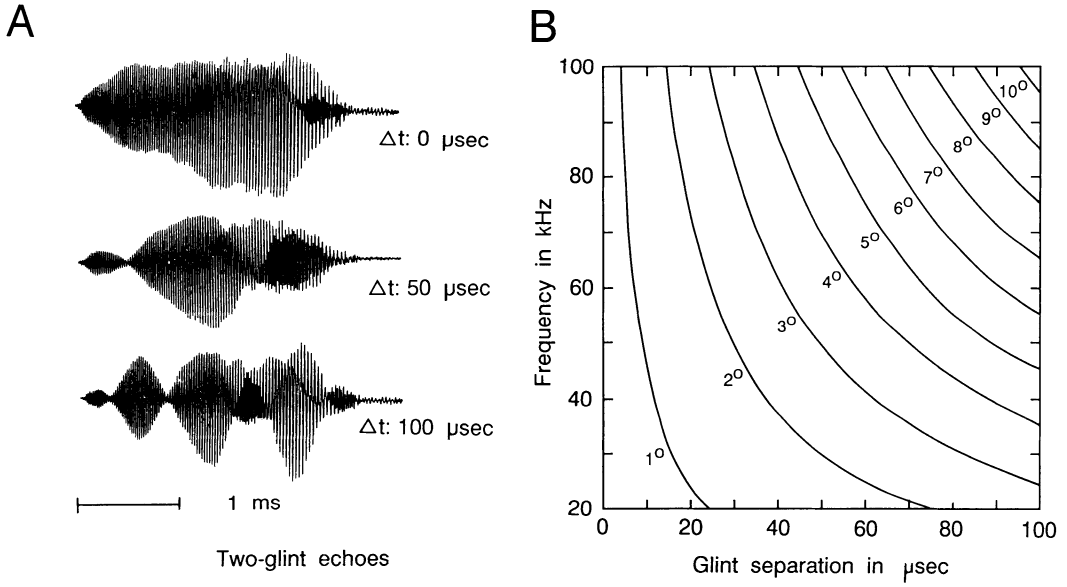

FIG. 21. Spectral representation of target range. *A*: waveforms of 3 multiple echoes of the same *Eptesicus* biosonar signal reflected from 2 surfaces (glints) separated by different ranges (time). As the separation time between the echoes increases (50 and 100 μs), the envelope of the signal becomes more rippled. Ripples in the waveforms are caused by interference patterns between the echoes reflected from the 2 glints. In particular, destructive interference causes the cancellation of certain frequencies, resulting in an amplitude minimum or spectral notch in the waveform. *B*: the family of hyperbolic curves shown in this graph illustrate the relationship between separation time of 2 glints and frequency of the spectral notches caused by the interference.

Schmidt 1988, 1992; Simmons et al. 1990), whereas absolute or coarse-range information is carried by the time delay between the emitted vocalization and the returning echo (Simmons 1971, 1973, 1989). Yet, behavioral results show that both types of range information are ultimately perceived as estimates of the range to the different parts of the target (Simmons et al. 1990). Thus fine- and coarse-range information converge onto the same perceptual axis of target range, presumably through the integration of their parallel auditory representations. This finding, coupled with the observation of overlapping tonotopic and delay-tuned cortical fields in *Myotis* (Wong and Shannon 1988), has lead to the suggestion that the pattern of overlapping tonotopic and delay-tuned fields contributes to the convergence of range cues in FM bats (Shannon-Hartman et al. 1992; Wong and Shannon 1988). The CF-FM bat *Rhinolophus* also exhibits overlapping tonotopic and delay-tuned cortical fields similar to *Myotis* (Schuller et al. 1991), but the limited range of the FM sweep used by this species makes it unlikely that it is encoding spectral notches. Our observations on cortical organization support this suggestion, and we offer a conceptual framework to interpret the cortical distributions of multipeaked frequency-tuned and delay-tuned neurons in *Eptesicus*.

If multipeaked frequency-tuned neurons play a functional role in encoding spectral notches in echoes, whereas delay-tuned neurons play a role in encoding echo delay, then perhaps the spatial overlap of the multipeaked frequency-tuned and delay-tuned fields may contribute to the demonstrated convergence of fine- and coarse-range information onto the same perceptual axis of target range. Specifically, this integration may require multipeaked frequency-tuned neurons to locally interact with different delay-tuned neurons covering a wide range of echo delays. Our data suggest that multipeaked frequency-tuned and delay-tuned neurons are separate populations because only 1 of the 39 multipeaked neurons exhibited any delay sensitivity, consistent with parallel pathways for encoding range information. In addition, the distribution of multipeaked frequency-tuned neurons, as illustrated in the composite multipeaked map (Fig. 9), almost completely overlaps the distribution of delay-tuned neurons except in the posterior, tonotopic portion of the auditory cortex, as illustrated in the composite delay-tuned map (Fig. 12). Also, there were no delay-tuned or multipeaked neurons found in the small tonotopically organized reversal area (Fig. 4, area C), first identified in a previous study (Jen et al. 1989).

Each region of auditory cortex in the tonotopic area (Fig. 12) that contains many delay-tuned neurons and is bounded by the 10-kHz isofrequency contours encompasses BDs of 4–24 ms. Thus ensembles of similar frequency-tuned neurons and multipeaked neurons are in close proximity to delay-tuned neurons encompassing a wide range of BDs. This arrangement may permit the combination of any one glint separation with a wide range of different echo delays, a situation encountered during pursuit of an insect. We conclude by recapitulating the fact that the conceptual framework is speculative, and much work remains to establish its validity as an organizational principle in *Eptesicus* and perhaps other species of FM bats.

We thank Dr. Cynthia F. Moss for help with the experimental work in this study, P. Saillant for collecting and providing the spectrogram data, F. Bouffard for technical support with preparation of the manuscript, and Dr. Andrea Megela Simmons for helpful comments on the text.

This research was supported by Office of Naval Research Grant N00014-89-J-3055, National Institute of Mental Health Grant MH-00521, and Training Grant MH-19118.

Address reprint requests to S. P. Dear.

Received 22 June 1992; accepted in final form 12 July 1993.

REFERENCES

ABELES, M. AND GOLDSTEIN, M. H. Functional architecture in cat primary auditory cortex: columnar organization and organization according to depth. *J. Neurophysiol.* 33: 172–187, 1970.

ARMSTRONG-JAMES, M. AND MILNAR, J. Carbon fibre microelectrodes. *J. Neurosci. Methods* 1: 279–287, 1979.

BERKOWITZ, A. AND SUGA, N. Neural mechanisms of ranging are different in two species of bats. *Hear. Res.* 41: 255–264, 1989.

BEUTER, K. J. A new concept of echo evaluation in the auditory system in bats. In: *Animal Sonar Systems*, edited by R.-G. Busnel and J. F. Fish. New York: Plenum, 1980, p. 747–761.

BRIGHAM, R. M., CEBEK, J. E., AND HICKEY, M. B. C. Intraspecific variation in the echolocation calls of two species of insectivorous bats. *J. Mammal.* 70: 426–428, 1989.

DEAR, S. P., HARESIGN, T., FERRAGAMO, M., FRITZ, J., MOSS, C., AND SIMMONS, J. Response properties of neurons in the auditory cortex of the big brown bat. *Soc. Neurosci. Abstr.* 20: 718, 1990.

EDAMATSU, H., KAWASAKI, M., AND SUGA, N. Distribution of combination sensitive neurons in the ventral fringe area of the auditory cortex of the mustached bat. *J. Neurophysiol.* 61: 202–207, 1989.

EVANS, E. F., ROSS, H. F., AND WHITFIELD, I. C. The spatial distribution of unit characteristic frequency in the primary auditory cortex of the cat. *J. Physiol. Lond.* 179: 238–247, 1965.

EVANS, E. F. AND WHITFIELD, I. C. Classification of unit responses in the auditory cortex of unanesthetized and unrestrained cat. *J. Physiol. Lond.* 171: 476–493, 1964.

FENG, A. S., SIMMONS, J. A., AND KICK, S. A. Echo detection and target-ranging neurons in the auditory system of the bat, *Eptesicus fuscus*. *Science Wash. DC* 202: 645–648, 1978.

GAIONI, S. J., RIQUIMAROUX, H., AND SUGA, N. Biosonar behavior of mustached bats swung on a pendulum prior to cortical ablation. *J. Neurophysiol.* 64: 1801–1817, 1990.

GALAMBOS, R. Studies of the auditory system with implanted electrodes. In: *Neural Mechanisms of the Auditory and Vestibular Systems*, edited by G. L. Rasmussen and W. F. Windle. Springfield, IL: Thomas, 1960, p. 137–151.

GOULD, E. Studies of maternal-infant communication and development of vocalizations in bats *Myotis* and *Eptesicus*. *Commun. Behav. Biol.* 5: 263–313, 1971.

GRIFFIN, D. R. *Listening in the Dark*. New Haven, CT: Yale Univ. Press, 1958. (Reprinted by Dover Publications, New York, 1974, and Cornell Univ. Press, Ithaca, NY, 1986.)

GRIFFIN, D. R. Comparative studies of the orientation sounds of bats. *Symp. Zool. Soc. Lond.* 7: 61–72, 1962.

GRIFFIN, D. R. The importance of atmospheric attenuation for the echolocation of bats (*Chiroptera*). *Anim. Behav.* 19: 55–61, 1971.

HABERSETZER, J. AND VOGLER, B. Discrimination of surface structured targets by the echolocating bat *Myotis myotis* during flight. *J. Comp. Physiol. A* 152: 275–282, 1983.

JEN, P. H. S. AND KAMADA, T. Analysis of orientation signals emitted by the CF-FM bat, *Pteronotus p. parnellii* and the FM bat, *Eptesicis fuscus* during avoidance of moving and stationary obstacles. *J. Comp. Physiol. A* 148: 389–398, 1982.

JEN, P. H. S., SUN, X., AND LIN, P. J. J. Frequency and space representation in the primary auditory cortex of the frequency modulating bat *Eptesicus fuscus*. *J. Comp. Physiol. A* 165: 1–14, 1989.

KICK, S. A. Target detection by the echolocating bat, *Eptesicus fuscus*. *J. Comp. Physiol. A* 145: 431–435, 1982.

KICK, S. A. AND SIMMONS, J. A. Automatic gain control in the bat's sonar receiver and the neuroethology of echolocation. *J. Neurosci.* 4: 2705–2737, 1984.

KOBER, R. AND SCHNITZLER, H. U. Information in sonar echoes of fluttering insects available for echolocating bats. *J. Acoust. Soc. Am.* 87: 882–895, 1990.

KOBLER, J. B., WILSON, B. S., HENSON, O. W., AND BISHOP, A. L. Echo intensity compensation by echolocating bats. *Hear. Res.* 20: 99–108, 1985.

KURTA, A. AND BAKER, R. H. *Eptesicus fuscus*. *Mamm. Species* 356: 1–10, 1990.

LAWRENCE, B. D. AND SIMMONS, J. A. Measurement of atmospheric attenuation at ultrasonic frequencies and the significance for echolocation by bats. *J. Acoust. Soc. Am.* 71: 484–490, 1982.

MASTERS, W. M., JACOBS, S. C., AND SIMMONS, J. A. The structure of echolocation sound used by the big brown bat *Eptesicus fuscus*: some consequences for echo processing. *J. Acoust. Soc. Am.* 89: 1402–1413, 1991.

MERZENICH, M. M., KNIGHT, P. L., AND ROTH, G. L. Representations of cochlea within primary auditory cortex in cat. *J. Neurophysiol.* 38: 231–249, 1975.

MOGDANS, J. AND SCHNITZLER, H.-U. Range resolution and the possible use of spectral information in the echolocating bat, *Eptesicus fuscus*. *J. Acoust. Soc. Am.* 88: 754–757, 1990.

O'NEILL, W. E. AND SUGA, N. Target range-sensitive neurons in the auditory cortex of the mustached bat. *Science Wash. DC* 203: 69–73, 1979.

O'NEILL, W. E. AND SUGA, N. Encoding of target-range information and its representation in the auditory cortex of the mustached bat. *J. Neurosci.* 2: 17–31, 1982.

OONISHI, S. AND KATSUKI, Y. Functional organization and integrative mechanism on the auditory cortex of the cat. *Jpn. J. Physiol.* 15: 342–365, 1965.

SAILLANT, P. A., SIMMONS, J. A., DEAR, S. P., AND MCMULLEN, T. A. A computational model of echo processing and acoustic imaging in FM echolocating bats: the SCAT receiver. *J. Acoust. Soc. Am.* In press.

SCHMIDT, S. Evidence for a spectral basis of texture perception in bat sonar. *Nature Lond.* 331: 617–619, 1988.

SCHMIDT, S. Perception of structured phantom targets in the echolocating bat, *Megaderma lyra*. *J. Acoust. Soc. Am.* 91: 2203–2223, 1992.

SCHULLER, G., O'NEILL, W. E., AND RADTKE-SCHULLER, S. Facilitation and delay sensitivity of auditory cortex neurons in CF-FM bats, *Rhinolophus rouxi* and *Pteronotus p. parnellii*. *Eur. J. Neurosci.* 3: 1165–1181, 1991.

SCHULLER, G., RADTKE-SCHULLER, S., AND O'NEILL, W. E. Processing of paired biosonar signals in the cortices of *Rhinolophus rouxi* and *Pteronotus parnellii*: a comparative neurophysiological and neuroanatomical study. In: *Animal Sonar Systems*, edited by P. E. Nachtigall and P. W. B. Moore. New York: Plenum, 1989, p. 259–264.

SHANNON-HARTMAN, S., WONG, D., AND MAEKAWA, M. Processing of pure-tone and FM stimuli in the auditory cortex of the FM bat, *Myotis lucifugus*. *Hear. Res.* 61: 179–188, 1992.

SIMMONS, J., FREEDMAN, E. G., STEVENSON, S. B., CHEN, L., AND WOHLGENANT, T. Clutter interference and the integration time of echoes in the echolocating bat, *Eptesicus fuscus*. *J. Acoust. Soc. Am.* 86: 1318–1332, 1989.

SIMMONS, J. A. The sonar receiver of the bat. *Ann. NY Acad. Sci.* 188: 161–174, 1971.

SIMMONS, J. A. The resolution of target range by echolocating bats. *J. Acoust. Soc. Am.* 54: 157–173, 1973.

SIMMONS, J. A. Perception of echo phase information in bat sonar. *Science Wash. DC.* 207: 1336–1338, 1979.

SIMMONS, J. A. Time-frequency transforms and images of targets in the sonar of bats. In: *Princeton Lectures in Biophysics*, edited by W. Bialek. River Edge, NJ, 1992, p. 291–319.

SIMMONS, J. A. A view of the world through the bat's ear: the formation of acoustic images in echolocation. *Cognition* 33: 155–199, 1989.

SIMMONS, J. A. AND CHEN, L. The acoustic basis for target discrimination by FM echolocating bats. *J. Acoust. Soc. Am.* 86: 1333–1350, 1989.

SIMMONS, J. A., MOSS, C. F., AND FERRAGAMO, M. Convergence of temporal and spectral information into acoustic images of complex sonar targets perceived by the echolocating bat, *Eptesicus fuscus*. *J. Comp. Physiol. A* 166: 449–470, 1990.

SIMMONS, J. A., SAILLANT, P. A., AND DEAR, S. P. Through a bat's ear. *IEEE Spectrum* 29: 46–48, 1992.

SUGA, N. The extent to which biosonar information is represented in the bat auditory cortex. In: *Dynamic Aspects of Neo-Cortical Function*, edited by G. M. Edelman, W. E. Gall, and W. M. Cowan. New York: Wiley, 1984, p. 315–373.

SUGA, N. What does single-unit analysis in the auditory cortex tell us about information processing in the auditory system? In: *Neurobiology of Neocortex*, edited by P. Rakic and W. Singer. New York: Wiley, 1988, p. 331–349.

SUGA, N. AND HORIKAWA, J. Multiple time axes for representation of echo delays in the auditory cortex of the mustached bat. *J. Neurophysiol.* 55: 776–805, 1986.

SUGA, N. AND MANABE, T. Neural basis of amplitude-spectrum representation in auditory cortex of the mustached bat. *J. Neurophysiol.* 47: 225–255, 1982.

SUGA, N. AND O'NEILL, W. E. Neural axis representing target range in the auditory cortex of the mustached bat. *Science Wash. DC* 206: 351–353, 1979.

SUGA, N., O'NEILL, W. E., KUJIRAI, K., AND MANABE, T. Specificity of combination sensitive neurons for processing of complex biosonar signals in the auditory cortex of the mustached bat. *J. Neurophysiol.* 49: 1573–1626, 1983.

SUGA, N., O'NEILL, W. E., AND MANABE, T. Cortical neurons sensitive to particular combinations of information-bearing elements of biosonar signals in the mustached bat. *Science Wash. DC* 200: 778–781, 1978.

SUGA, N. AND SCHLEGEL, P. Neural attenuation of response to emitted sounds in echolocating bats. *Science Wash. DC* 177: 82–84, 1972.

SUGA, N. AND SHIMOZAWA, T. Site of neural attenuation to self-vocalized sounds in echolocating bats. *Science Wash. DC* 183: 1211–1213, 1974.

SUGA, N. AND TSUZUKI, K. Inhibition and level-tolerant frequency tuning in the auditory cortex of the mustached bat. *J. Neurophysiol.* 53: 1109–1145, 1985.

SULLIVAN, W. E. Neural representation of target distance in auditory cortex of the echolocating bat *Myotis lucifugus*. *J. Neurophysiol.* 48: 1011–1032, 1982.

SUTTER, M. L. AND SCHREINER, C. E. Physiology and topology of neurons with multipeaked tuning curves in cat primary auditory cortex. *J. Neurophysiol.* 65: 1207–1226, 1991.

TANIGUCHI, I., NIWA, H., WONG, D., AND SUGA, N. Response properties of FM-FM combination-sensitive neurons in the auditory cortex of the mustached bat. *J. Comp. Physiol. A* 159: 331–337, 1986.

TENG, H. AND WONG, D. Dual amplitude sensitivity of delay-sensitive neurons in the auditory cortex of *Myotis lucifugus*. *ARO Abstr.* 15: 423, 1992.

THOMAS, D. W., BELL, G. P., AND FENTON, M. B. Variation in echolocation call frequencies recorded from North American vespertilionid bats: a cautionary note. *J. Mammal.* 68: 842–847, 1987.

WONG, D., MAEKAWA, M., AND TANAKA, H. The effect of pulse repetition rate on the delay-sensitivity of neurons in the auditory cortex of the FM bat, *Myotis lucifugus*. *J. Comp. Physiol. A* 170: 393–402, 1992.

WONG, D. AND SHANNON, S. L. Functional zones in the auditory cortex of the echolocating bat, *Myotis lucifugus*. *Brain Res.* 453: 349–352, 1988.